

AN ABSTRACT OF THE DISSERTATION OF

Hasini R. Perera for the degree of Doctor of Philosophy in Chemistry presented on May 26, 2009

Title: Galvanostatic Control of Ion Selective Electrodes with the Solvent Polymeric Membrane.

Abstract approved:

Alexey Y. Shvarev

Detection technique that proposed utilizing electrochemically controlled, reversible ion extraction into polymeric membrane in an alternating galvanostatic/ potentiostatic mode was introduced. This method is studied in detail to comprehend the advantages of the novel sensor (pulstrode) compared to the potentiometric ion selective electrode (ISE), studies included possible applications and limitations.

Solvent polymeric membrane of the pulstrode contains a highly lipophilic electrolyte and, therefore does not possess spontaneous ion exchange properties. As a consequence pulstrodes have the ability to determine unbiased selectivity coefficients without the careful counterbalancing of transmembrane ionic fluxes. In contrast to classical ISEs they work under asymmetric conditions. Therefore pulstrodes offer simplicity in the determination of selectivity and the results obtained are prone to less error. Further studies with K^+ , Ag^+ and Ca^{2+} selective electrodes reveal that pulstrodes yield the same or slightly favorable unbiased selectivity coefficients than the previously reported literature values. Since pulstrodes were demonstrated as reliable sensor to determine unbiased selectivity of neutral carriers, they were used to screen potential anion carriers. Selectivity coefficients for [12]-Mercuracarborand-4 was determined using pulstrodes as well as classical ISEs indicating that it has high selectivity towards I⁻. MC4 may be the most selective I⁻ carrier known to date.

Ultimately various aspects of the development of reliable, robust and comparatively maintenance free solid contact sensors using conducting polymer as the transduction layer were considered on a model system. Sodium selective pulstrodes based on poly(3,4-ethylendioxythiophene)-poly(styrene sulfonate) (PEDOT:PSS) was identified as the best performing sensor and a protamine selective solid contact pulstrode was fabricated using PEDOT:PSS as the transduction layer. This solid contact pulstrode exhibit a substantial improvement of the low detection limit (0.03 mg/L).

© Copyright by Hasini R. Perera

May 26, 2009

All Rights Reserved

Galvanostatic Control of Ion Selective Electrodes with the Solvent Polymeric
Membrane.

by

Hasini R. Perera

A DISSERTATION

Submitted to

Oregon State University

In partial fulfillment of

the requirements for the

degree of

Doctor of Philosophy

Presented May 26, 2009

Commencement June 2010

Doctor of Philosophy dissertation of Hasini R. Perera
Presented on May 26, 2009

APPROVED:

Major Professor, representing Chemistry

Chair of the Department of Chemistry

Dean of the Graduate School

I understand that my dissertation will become part of the permanent collection of Oregon State University libraries. My signature below authorizes release of my dissertation to any reader upon request.

Hasini R. Perera, Author

ACKNOWLEDGEMENTS

I'm deeply indebted to my research advisor, Dr. Alexey Shvarev for his guidance and support throughout my graduate carrier. I appreciate his enthusiasm in my work and stimulating suggestions that helped to improve the quality of this work.

A sincere thank you is also extended to Dr. John Westall for providing invaluable suggestions and guidance throughout the course of study. I appreciate the time and commitment of my graduate committee members, Dr. Vincent Remcho, Dr. Michael Lerner, Dr. David Hakleman and Dr. John Westall.

During my stay at OSU, I was fortunate to work with an excellent group of people. My special thanks go to all Shvarev group members, Katy Fordyce, Valeriya Bychkova, Natalia Pilipiuk and Dustin Quandt for their friendship and advice. Especially I appreciate the excellent suggestions given by Katy during proof reading of the manuscript.

I thank my many friends for cheerfully tolerating my joyful and sorrowful natures equally. Particularly I thank Myra Koesdjojo, Yolanda Tennico, Jintana Nammoonnoy, Esha Chatterjee, Sharmistha Nag, Sumitra Sengupta and Tae Hyeong Kim for their moral support throughout the years.

I extend my gratitude to the faculty and staff of Department of Chemistry, OSU.

I acknowledge with gratitude Jim & Debo Richman and Joan & Keith Dunlap for making the transition from Sri Lanka to Corvallis a pleasant experience. Also I appreciate the Sri Lankan community in Corvallis, who provided a familiar home-style environment in a foreign country.

Last but not least I wish to thank my family, my parents for their endless love, encouragement and confidence in me. I'm very grateful to my husband, Suranga for his love, understanding and support.

CONTRIBUTION OF AUTHORS

Dr. Alexey Shvarev provided major assistance in interpreting data, editing and writing this dissertation. In Chapter 5, Katherine Fordyce obtained the time-dependent response of protamine-selective PEDOT:PSS solid-contact sensor.

TABLE OF CONTENTS

	<u>Page</u>
1. Introduction	1
1.1 History.....	2
1.2 Pulsed Chronopotentiometric Sensors (Pulstrodes).....	3
1.3 Unbiased Selectivity.....	5
1.3.1 Use of ion buffers in sample solution/inner filling Solution	6
1.3.2. Use of membranes that are conditioned with an interfering ion.....	6
1.3.3. Use of the pulstrodes	7
1.4 New membrane components	7
1.4.1. Selectivity studies	9
1.4.2 Complex stability studies	9
1.5 Solid Contacts	10
1.6 References	14
2. Unbiased Selectivity Coefficients Obtained for the Pulsed Chronopotentiometric Polymeric Membrane Ion Sensors	15
2.1 Abstract	16
2.2 Communication.....	17
2.3 Supporting Information.....	22
2.4 References	25
3. Determination of Unbiased Selectivity Coefficients using Pulsed Chronopotentiometric Polymeric Membrane Ion Sensors	26
3.1 Abstract	27
3.2 Introduction	27

TABLE OF CONTENTS (Continued)

	<u>Page</u>
3.3 Experimental Section	29
3.3.1 Reagents	29
3.3.2 Membrane Preparation	29
3.3.3 Liquid-contact electrodes	30
3.3.4 Chronopotentiometric measurements	30
3.4 Results & Discussion	31
3.5 Conclusions	42
3.6 Acknowledgment	43
3.7 References	44
4. Characterization of [12]-Mercuracarborand-4 : An Ionophore with Iodide complexing cavity.....	46
4.1 Abstract	47
4.2 Introduction	47
4.3 Experimental	49
4.3.1 Reagents	49
4.3.2 Ion Selective Membrane Preparation	50
4.3.3 Liquid-contact electrodes	50
4.3.4 Chronopotentiometric measurements	50
4.3.5 Potentiometric Measurements.....	51
4.3.6 Optode Film Preparation.....	51
4.3.7 Sample Preparation for Optical Measurements.....	52
4.3.8 Fluorescence Measurements	52
4.3.9 Stability Constant Measurements.....	53
4.4 Results & Discussion	53
4.5 Conclusion	62

TABLE OF CONTENTS (Continued)

	<u>Page</u>
4.6 Reference.....	63
5. Pulsed Galvanostatic Control of Solid-State Polymeric Ion-Selective	
Electrodes	64
5.1 Abstract	65
5.2 Introduction	65
5.3 Experimental Section	69
5.3.1 Reagents	69
5.3.2 Membrane Preparation	69
5.3.3 Liquid-contact electrodes	70
5.3.4 Solid-contact electrodes	70
5.3.5 Chronopotentiometric measurements	71
5.3.6 Electrochemical Impedance Measurements	72
5.4 Theoretical Section.....	72
5.4.1 Liquid contact interface.....	73
5.4.2 Solid contact interface with a conducting polymer as a transducer	77
5.5 Results and Discussion.....	81
5.6 Conclusions.....	93
5.7 Acknowledgement.....	94
5.8 References	95
6. Conclusion and Future Aspects.....	97
7. Appendix A	102

LIST OF FIGURES

<u>Figure</u>	<u>Page</u>
1.1 Time profile of a triple pulse experiment to control the pulstrodes.....	4
1.2 Structures of Mercuracarborand ionophores.....	8
1.3 Schematic representation of the two-layer sandwich method to determine the complex formation constants in solvent polymeric membranes	9
1.4 Layout of a solid contact sodium selective pulstrode with poly (3,4-ethylenedioxythiophene) (PEDOT) doped with immobilized poly(styrene sulfonate) (PSS) acting as the ion-to-electron Transducer.....	12
2.1 Response of K-selective pulstrodes towards chloride salts of K and Mg	19
2.2 Response of K-selective potentiometric electrodes conditioned in A) 0.01 M NaCl	21
3.1 Schematic representation of concentration gradients of the primary ions in (A) traditional potentiometric ISE.....	32
3.2 Response of K-selective pulstrodes towards chloride salts of K ⁺ (slope 60.0 mV/dec).....	36
3.3 Experimental selectivity coefficients, ($\log K_{K,J}^{pot}$) for (A) K-selective PVC-o-NPOE (1:2) pulstrode membranes containing valinomycin and ETH 500	36
3.4 Response of Ag-selective pulstrodes towards nitrate salts of Ag ⁺ (slope 50.4 mV/dec).....	38
3.5 Experimental selectivity coefficients, ($\log K_{Ag,J}^{pot}$) for (A) Ag-selective PVC-oNPOE (1:2) pulstrode membranes containing MBDiBTC and ETH 500.....	39
3.6 Response of Ca-selective pulstrodes towards chloride salts of Ca ²⁺ (slope 29.5 mV/dec).....	40

LIST OF FIGURES (Continued)

<u>Figure</u>	<u>Page</u>
3.7 Experimental selectivity coefficients, ($\log K_{Ca,J}^{pot}$) for (A)Ca-selective PVC-o-NPOE (1:2) pulstrode membranes containing MBDiBTC and ETH 500	41
4.1 Chemical structure of Mercuracarborand ionophores.....	48
4.2 Response of pulstrode containing MC3 carrier, towards K^+ salts of I^- (slope = -59.04 mV/dec)	54
4.3 Experimental selectivity coefficients, ($\log K_{I,J}^{pot}$) for (A) I-selective PVC:o-NPOE (1:2) pulstrode membranes containing MC3 and ETH500 potentials measured under zero current conditions	55
4.4 Response of pulstrode containing MC4 carrier, (A) conditioned in 0.01 M NaCl.....	58
4.5 Experimental selectivity coefficients, ($\log K_{I,J}^{pot}$) for (A) I-selective PVC:o-NPOE (1:2) pulstrode membranes containing MC3 and ETH500 potentials measured under zero current conditions	62
5.1 Schematic representation of the concentration gradients induced by a cathodic current applied across the sodium selective-membrane	74
5.2 Pulsed chronopotentiograms for a sodium-selective membrane containing lipophilic electrolyte ETH 500 and sodium ionophore in separate solutions of 0.01 M KCl, NaCl, LiOAc, $CaCl_2$ and $MgCl_2$	82
5.3 Response to sodium in presence of 0.01 M $MgCl_2$ at constant current of -7 μA , the pulse duration is 1 s.....	83
5.4 Potential stability of the PEDOT:PSS solid-contact sensor	86
5.5 Time-dependent response of the sodium calibration	87
5.6 Impedance spectra in 0.01M NaCl in presence of 0.01M $MgCl_2$ background electrolyte	88

LIST OF FIGURES (Continued)

<u>Figure</u>	<u>Page</u>
5.7 The total potential drift of the PEDOT:PSS solid-contact sensor as a function of the duration of the applied current pulse of $-6 \mu\text{A}$ and ETH500 concentration in the membrane	91
5.8. Time-dependent response of protamine-selective PEDOT:PSS solid-contact sensor in the solution of 0.1 M NaCl and 50 mM TRIS, pH 7.40.	92

LIST OF TABLES

<u>Table</u>	<u>Page</u>
5.1 Optimum logarithmic selectivity coefficients ($\log K_{Na,J}^{pot}$) obtained for sodium-selective galvanostatically controlled ion-selective sensors (pulstrodes).....	84
5.2 Results from impedance measurements (frequency range 100 kHz - 10 mHz).....	89

LIST OF APPENDIX FIGURES

<u>Figure</u>	<u>Page</u>
A.1 Slopes obtained for the calibration curves of Na ⁺ , Ca ²⁺ and H ⁺ pulstrodes, at different currents as a function of the applied current	104
A.2 Slope obtained for calibration plot of ionophore free pulstrode membrane as a function of the applied current	105

CHAPTER 1

INTRODUCTION

1.1 History

Ion selective electrodes (ISEs) remain the oldest class of chemical sensors, with the discovery of pH response of thin glass membranes by Cremer in 1906. However, the first commercial ISE, a glass pH electrode was developed more than two decades later in 1932 by Arnold Beckman. Glass pH electrodes still remain the most widespread sensors used in virtually any laboratory. Although the performance of the best glass and crystalline membranes remain unsurpassed, the chemical versatility of these materials is limited, which imposes restrictions on the range of available analytes.

Many fixed site ion exchange membranes were developed following the discovery of sulfonated polystyrene. These membranes have general potentiometric response for many cations and anions and are useful as general ion sensors. However, the membranes often suffer from insufficient selectivity, which is based on the Hofmeister sequence of ions. A breakthrough in ISE technology came with the discovery of valinomycin as a neutral carrier (ionophore) in 1966. A remarkable improvement of sensor selectivity was observed as a result of incorporating an ionophore into the membrane. Electrodes that incorporated valinomycin measured K^+ in presence of 5000 fold excess of Na^+ . This was significant for clinical and environmental applications where the samples often contain high concentrations of interfering ions. The intuitive work of designing new, highly selective ionophores, following the discovery of valinomycin have made the ionophore based sensors quite successful.

Another important contribution to the success of ISEs, came with the introduction of liquid, polymer matrix membranes impregnated with ion selective components (solvent polymeric membranes) by Shatkay and co-workers¹. After its initial introduction, plasticized poly(vinyl chloride) (PVC) membranes were quickly and widely received. Even though the use of many other polymers such as poly(styrene), poly(methyl methacrylate), poly(vinyl butyl), poly(amide) and poly(imide) have been demonstrated, PVC still remains the most widely used matrix for the ISEs. Following these discoveries, ionophore based solvent polymeric membrane sensors became the

most successful class among ISEs². Therefore, the field of ISEs as we know it developed during the 1960s³.

The great success ISEs have achieved during the past decade has not converted the field into a stagnating mature discipline. Recently, a new direction in the field of ISEs has emerged with the development of potentiometric sensors for the detection of polyionic macromolecules⁴. The electrode's response to highly charged polyions has been attributed to a non-equilibrium, quasi-steady-state change in the phase boundary potential at membrane/sample interface rather than the classical equilibrium approach. Unfortunately, as a result of the strong binding and lipophilic interactions, polyions tend to accumulate in the membrane phase. Therefore strong, potential drifts are normally observed and sensor loses its response after relatively short exposure times. Further, extracted polyions can only be removed from the membrane by reconditioning in a concentrated solution of NaCl.

New transduction principles for solvent polymeric membranes were discovered which can overcome the drawbacks of classical potentiometric method. A new technique with instrumental control over the ion flux to and from the membrane has been introduced by Bakker *et al*⁵. The work, described here, is based on pulsed galvanostatic control of the ionophore based polymeric sensors with no intrinsic ion exchange properties.

1.2 Pulsed Chronopotentiometric Sensors (Pulstrodes)

Pulstrodes are ionophore based sensors which lack spontaneous ion exchange properties. The solvent polymeric membrane incorporated in the sensor contains tetradodecylammonium tetrakis(4-chlorophenyl)borate (ETH 500), a highly lipophilic electrolyte and ionophore embedded within the PVC matrix. A plasticizer is added to the membrane to lower the glass transition temperature (T_g) of the polymer. Lowering the T_g increases the elasticity and ensures sufficient ionic mobility in the membrane.

The experimental cell includes a three electrode electrochemical cell with a liquid contact membrane electrode in contact with internal Ag/AgCl electrode acting as the working electrode. Ion extraction/stripping is electrochemically controlled by an alternating galvanostatic/potentiostatic mode. A typical time profile of a pulstrode experiment is illustrated in Figure 1.1.

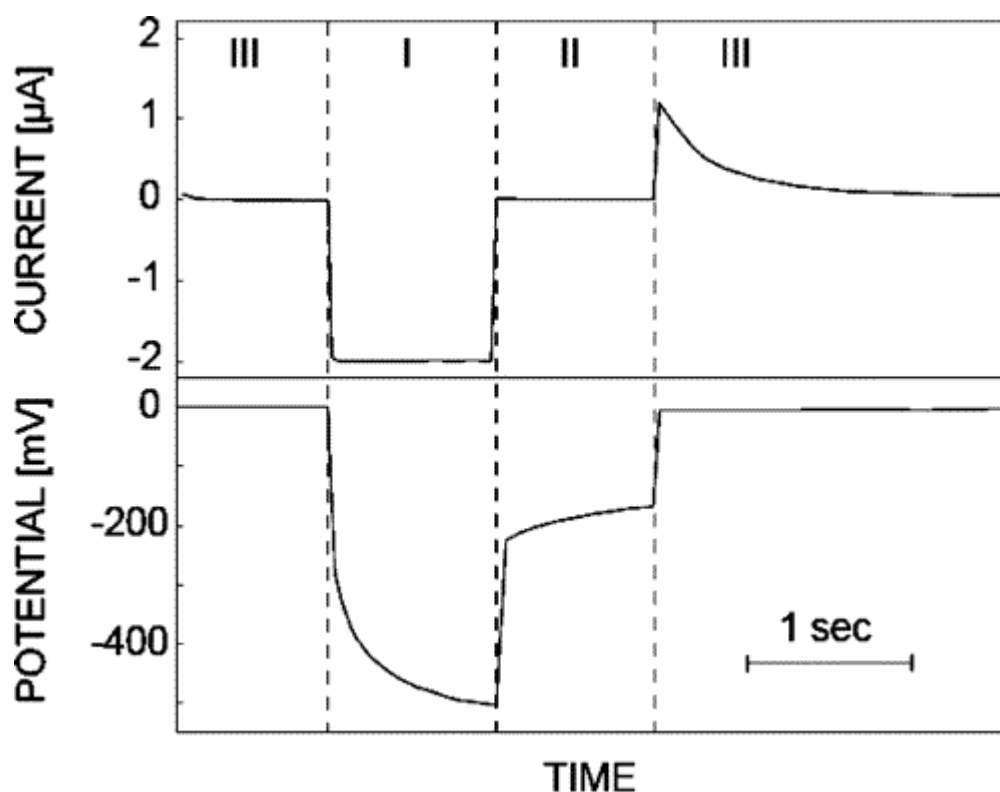


Figure 1.1 Time profile of a triple pulse experiment of a pulstrode⁶. Measured potential is with respect to a Ag/AgCl reference electrode.

In the galvanostatic mode, an initial current pulse (I) is followed by a zero current pulse (II). Pulse I has complete control over the magnitude and the sign of the ion flux into the membrane. During this pulse analyte ions (hereinafter referred to as the primary ion) as well as background ions get extracted into the membrane. During pulse II, previously extracted background ions are allowed to exchange with the primary ion. All extracted ions are expelled from the membrane during the baseline potential pulse (III, Potentiostatic mode), thus regenerating the membrane for the next measurement. Furthermore, it has been found that the integrated area under the current

pulse I is equal to the area under the current produced in phase III. This confirms that it is possible to yield a reproducible sensor on the basis of a chemically irreversible reaction. It has been found that the duration of the stripping potential has to be at least 10 times longer than the current pulse⁶. Potentials are monitored during discrete time intervals (last 10%) of the applied current pulse and the zero current pulse. Potential monitored at the end of the zero current pulse is analogous to that observed in potentiometric ISEs, without any effect of the iR drop across the membrane.

This method can be applied not only for polyion detection but also for the detection of small ions as well^{5,7,8}. An attractive feature of the pulstrode response is that it mimics the potentiometric ISE behavior. Therefore, its response can be elucidated through well studied ISE theory. Furthermore, the pulstrode results can be compared against the published potentiometric results.

1.3 Unbiased Selectivity

An essential property of a sensor is its selectivity. Various methods for the determination of ISE selectivity coefficients have been described in the literature². A frequent practical error in the determination of selectivity is that it is determined when a non-Nernstian electrode slope is observed for ions that exhibit less affinity towards the ionophore. (hereinafter referred to as discriminated ions) Typically, such problems arise when discriminated ion solutions carry impurities of primary ions. A major source of contamination is the flux of primary ions from the membrane to the sample, creating a nonzero primary ion level at the membrane surface which partly or completely dictates the electrode response. As a consequence, the resulting selectivity coefficients may be biased by many orders of magnitude^{9,10}.

A number of research groups have developed measures to eliminate the transmembrane ion flux and thus determine the unbiased thermodynamic selectivity coefficients of neutral ionophores.

1.3.1 Use of ion buffers in sample solution/inner filling solution.

Chelates of the primary ion such as ethylenediaminetetraacetic acid (EDTA) and Nitritotriacetic acid (NTA) are introduced into a solution of a discriminated ion that is being measured^{11, 12}. These can immediately buffer the primary ions that have been introduced as impurities of the calibration solution or have leached from the membrane into the sample to a very low concentration level. Therefore discriminated ions can displace the primary ions completely from the phase boundary region of the electrode so that a Nernstian slope is obtained for the discriminated ion.

Another approach towards obtaining unbiased selectivity is to prevent primary ions from leaching into the sample by building up a concentration gradient in the membrane^{13, 14}. The gradient is established by choosing an inner filling solution (IFS) with a low primary ion activity and sufficiently high discriminated ion activity. This induces a constant flux of primary ions towards the IFS, allowing the complete displacement of primary ions from the membrane, thus, a Nernst slope for the discriminated ions. Low primary ion activity in the IFS is maintained using chelates.

These long and tedious procedures require careful optimization of the sample solution or the IFS depending on the ion of interest. In addition, these procedures can be utilized if only the primary ion can be buffered, while the discriminated ion is not. Furthermore, chelating ligands are available only for few ions, thus, the applicability of the method is limited.

1.3.2. Use of membranes that are conditioned with a discriminated ion.

A general method for determination of unbiased selectivity was introduced by Bakker^{9, 10}. This method requires avoiding exposure to primary ion prior to measuring discriminated ions. Therefore, the membranes are conditioned with a discriminated ion and then selectivity is determined in the order of increasing preference of the ions. This method yields Nernstian electrode slopes for highly discriminated ions and thereby unbiased selectivity coefficients.

However, this method has several major drawbacks. First, once a membrane is exposed to primary ions, it no longer responds to discriminated ions in a Nernstian manner. In addition, prior knowledge of the selectivity pattern of the ions is essential for testing. Furthermore, if a testing solution is slightly contaminated with primary ions, the selectivity coefficients will be affected drastically.

1.3.3. Use of the pulstrodes.

In this work, pulstrodes are introduced as a convenient tool in determining unbiased thermodynamic selectivity coefficients of neutral ionophores. The procedure for the determination of unbiased selectivity, which was put forth by Bakker^{9, 10} is reviewed here. Unbiased selectivity of the valinomycin ionophore towards Na^+ and Mg^{2+} with respect to K^+ are compared using the two methods in order to validate and discuss the advantage of the new method over the established method.

Furthermore this novel, simple method is presented as a general procedure to characterize the selectivity of cation carrier based pulstrodes. The general utility of the method is established experimentally with a variety of carriers.

1.4 New membrane components

Substantial research efforts have focused on the development of highly selective ionophores. Though remarkable advancements have been reached in cation selective ionophores, anion carriers are far less developed. The slow development of anion selective ionophores can be attributed to the diversity of the geometry of anions, comparatively larger size and the weaker hydration layer when compared to cations of the same size or charge¹⁵.

Less than a decade ago, Bachas *et al* introduced highly selective chloride carriers based on a new class of macrocyclic hosts, Mercuracarborands¹⁶. These carriers consist of carborane cages with the backbone connected through mercury centers. This

provides Lewis acid character to compound, thus forming a host for anions (Figure 1.2). The cavity size of these compounds are larger than the cationic macrocyclic systems, therefore anions are easily accommodated. More importantly, they can be functionalized with bulky, lipophilic electron withdrawing or electron donating groups with varying cavity sizes¹⁷. As a consequence tailored ionophores can be obtained for the anion of interest.

(1)

(2)

Figure 1.2 Structures of Mercuracarborand ionophores: (1) MC3 (2)MC4

It is well known that the selectivity of a macrocyclic ionophore is based on the “best fit” concept, related to the size of the cavity and the size of the ion of interest. Hawthorne *et al*¹⁷, who originally synthesized the chloride carrier, [9]-Mercuracarborand-3 (MC3), has synthesized a tetrameric cyclic host, [12]-Mercuracarborand-4 (MC4). With the use of x-ray diffraction studies they observed that the distance among Hg-x⁻ (x⁻ = Cl⁻, I⁻) is even shorter than the Van der Waals distance predicting excellent bonding possibilities with halides. Therefore, MC4 is tested herein, to evaluate its capability as an anion carrier. MC4 is characterized using selectivity and complex stability studies.

1.4.1. Selectivity studies

The determination of unbiased selectivity using pulstrodes, illustrated above in 1.3.3, is utilized. Selectivity coefficients obtained are validated using traditional ISEs that are conditioned with the discriminated ion. (1.3.2)

1.4.2 Complex stability studies

The sandwich membrane method was originally proposed by Mokrov and co-workers¹⁸ and later critically evaluated by Mikhelson *et al*¹⁹ and Bakker *et al*^{20, 21}. In this method, the two phase boundary potentials are uncoupled by fusing two membranes, one with ionophore and the other without, forming a sandwich. (Figure 1.3)

If contacting aqueous solutions are of identical composition, the membrane potential is a direct function of the activity ratio in both membrane segments. The ionophore in one segment would decrease the activity of ions in that segment remarkably compared to the other. The measured potential difference of the sandwich membrane and the membrane carrying no ionophore is used to calculate the complex formation constant.

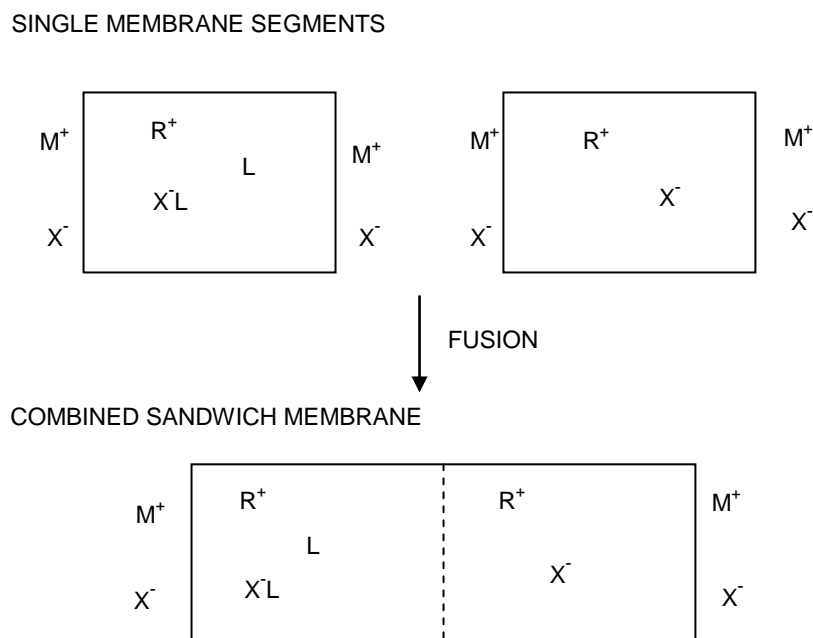


Figure 1.3 Schematic representation of the two-layer sandwich method to determine the complex formation constants in solvent polymeric membranes. Individual membrane segments are separately conditioned and their membrane potentials confirmed to be equivalent before combining them to form the sandwich membrane. The resulting membrane potential reflects the organic ion activity ratio at both interfaces. The symbol L, R⁺ and X⁻ indicate the ionophore, ionic site additives and anion respectively. The squares symbolize the membrane.

1.5 Solid Contacts

The ability of a pulstrode to obtain the true thermodynamic selectivity of an ionophore makes it a good candidate in clinical analysis. However, the presence of an inner filling solution could be a serious limitation in developing a reliable, robust and maintenance free sensor. An inner filling solution could limit the temperature range in sensor operation and give rise to undesired ionic fluxes in the membrane. Furthermore, miniaturization of the sensor is hindered.

Research groups have focused on substituting the inner filling solution and the internal reference electrode with a solid electron conducting substrate since the early 1970s. The invention of the coated wire electrode in 1971 was an important step towards solid state ISEs²². Although sensitivity and selectivity of these sensors were similar to the conventional ISE, they suffered from potential drifts due to poorly defined ion-to-electron transduction, resulting in poor reproducibility.

Conducting polymers (CPs) were later introduced as potential solid contacts due to their unique electrochemical properties such as electron conductivity, redox capacitance and ion exchange capability²³⁻²⁵. The reversible redox reactions in the CP are called p-doping (oxidation) and n-doping (reduction). The partially oxidized/reduced CP is accompanied by a doping anion/cation. The ion exchange property of the material can be altered significantly by changing the doping ion. Therefore the early reports on use of CPs in electrochemical sensors were focused on application of CPs as alternative to an ion selective membrane. However, due to interference caused by the presence of redox reactants in solution, sample pH changes and poor selectivity, this approach was not successful. In the second approach, the CP is electrodeposited or drop cast onto an electrical conductor. The ion selective membrane is then glued to the surface of the CP. The selectivity is governed by the ion selective membrane while the CP acts as the ion-to-electron transducer. Unlike coated wire electrodes, CPs demonstrate well defined ion-to-electron transduction pathways (Figure 1.4) and the high redox capacitance of the CP was found to stabilize the electrode potential. Therefore, the solid contact electrodes based on CPs in combination with ion selective membranes have been the most successful among solid contact ISEs.

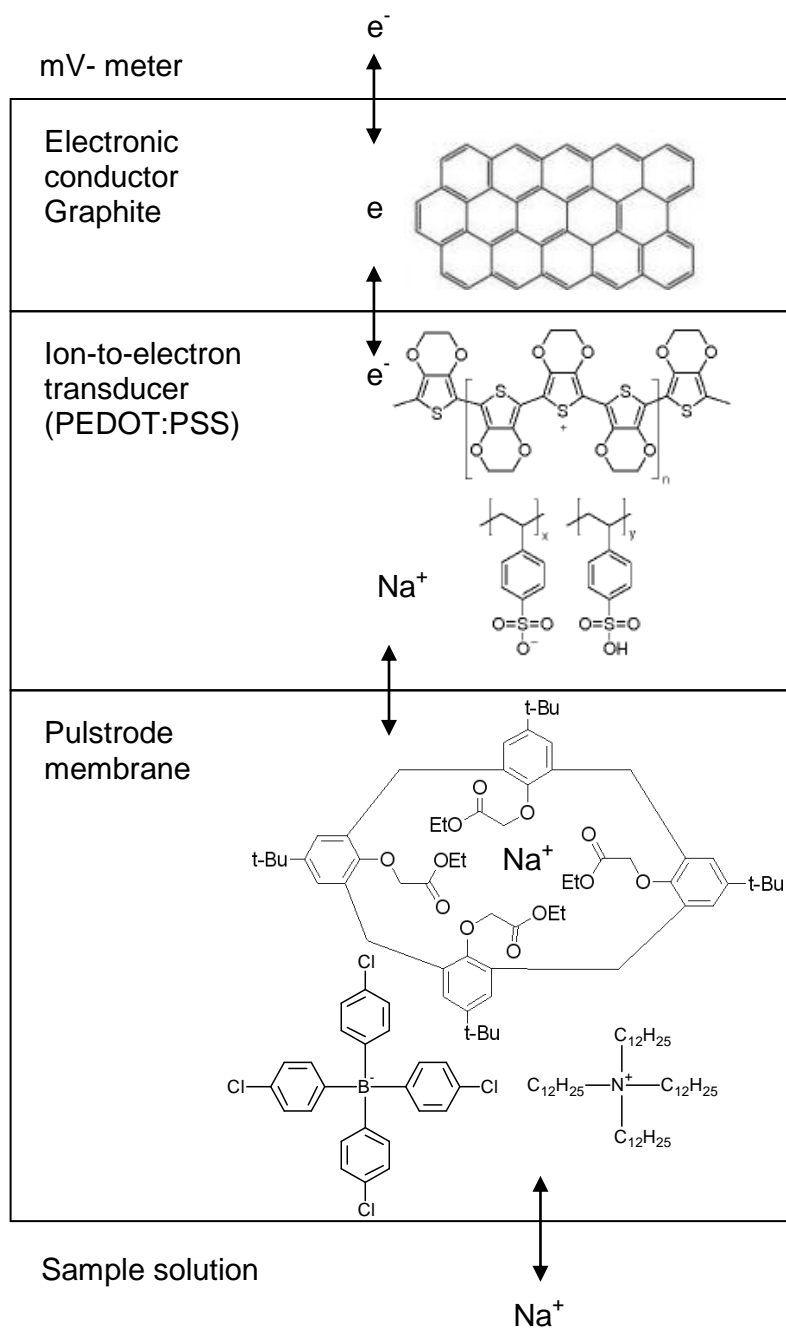


Figure 1.4 Layout of a solid contact sodium selective pulstrobe with poly(3,4-ethylenedioxythiophene) (PEDOT) doped with immobilized poly(styrene sulfonate) (PSS) acting as the ion-to-electron transducer

Herein, we focus on various aspects of the development of solid contact pulstrodes utilizing CPs. Sodium pulstrodes were studied as a sample system. The selectivity, short and long term stability and impedance analysis of the different CP systems were studied. The ultimate goal of this study is to fabricate a pulstrode using CPs as a transduction layer that can monitor biologically important polyionic macromolecules. Protamine is a low molecular weight protein (average M_r 4500 Da), which is administered routinely to patients following cardiovascular surgical procedures to neutralize the anticoagulant activity. The CP system that produced the best results in previous studies was used here to successfully fabricate a pulstrode that could monitor protamine. This represents the next step towards commercially viable polyion sensing technology.

1.6 References

- (1) Bloch, R.; Shatkay, A.; Saroff, H. A. *Biophysical Journal* **1967**, *7*, 865-877.
- (2) Bakker, E.; Buhlmann, P.; Pretsch, E. *Chem. Rev.* **1997**, *97*, 3083 - 3132.
- (3) R. P. Buck, E. L. *Anal. Chem.* **2001**, 88.
- (4) Fu, B.; Bakker, E.; Wang, E.; Yun, J. H.; Yang, V.; Meyerhoff, M. E. *Electroanalysis* **1995**, *7*, 823-829.
- (5) Shvarev, A. B., E. *Anal Chem* **2003**, *75*, 4541-4550.
- (6) Makarychev-Mikhailov, S., Shvarev, A., Bakker, E. *J. Am. Chem. Soc.* **2004**, *126*, 10548 - 10549.
- (7) Shvarev, A.; Bakker, E. *J. Am. Chem. Soc* **2003**, *125*, 11192-11193.
- (8) Shvarev, A.; Bakker, E. *Anal Chem* **2005**, *77*, 5221-5228.
- (9) Bakker, E. *J. Electrochem. Soc.* **1996**, *143*, L83 - L85.
- (10) Bakker, E. *Anal. Chem.* **1997**, *69*, 1061-1069.
- (11) Sokalski, T.; Maj-Zurawska, M.; Hulanicki, A. *Mikrochim. Acta* **1991**, *1*, 285-291.
- (12) Bakker, E.; Buhlmann, P.; Pretsch, E. *Electroanalysis* **1999**, *11*, 915 - 933.
- (13) Sokalski, T.; Ceresa, A.; Zwickl, T.; Pretsch, E. *J. Am. Chem. Soc.* **1997**, *119*, 11347-11348.
- (14) Sokalski, T.; Ceresa, A.; Fibbioli, M.; Zwickl, T.; Bakker, E.; Pretsch, E. *Anal. Chem.* **1999**, *71*, 1210 - 1214.
- (15) Antonisse, M. M. G.; Reinhoudt, D. N. *Electroanalysis* **1999**, *11*, 1035-1048.
- (16) Badr, I. H. A.; Diaz, M.; Hawthorne, M. F.; Bachas, L. G. *Anal. Chem.* **1999**, *71*, 1371-1377.
- (17) Hawthorne, M. F. Y., X; Zheng, Z. *Pure & Appl. Chem.* **1994**, *66*, 245-254.
- (18) Morkov, S. B.; Stefanova, O. K.; Materova, E. A.; Ivanova, E. E. *Vestn. Linangrad Univ.* **1984**, *16*, 41.
- (19) Shultz, M. M. S., O.K.; Mokrov, S.B.; Mikhelson, K.N *Anal. Chem.* **2002**, *74*, 510-517.
- (20) Mi, Y. B., E. *Anal Chem* **1999**, *71*, 5279-5287.
- (21) Qin, Y. M., Y.; Bakker, E. *Anal. Chim. Acta* **2000**, *421*, 207-220.
- (22) Cattrall, R. W.; Freiser, H. *Anal. Chem.* **1971**, *43*, 1905-1906.
- (23) Bobacka, J. *Electroanalysis* **2006**, *18*, 7-18.
- (24) Bobacka, J.; Lindfors, T.; Lewenstam, A.; Ivaska, A. *American Laboratory* **2004**, 13-20.
- (25) Michalska, A. *Anal. Bioanal. Chem.* **2006**, *384*, 391 - 406.

CHAPTER 2

**UNBIASED SELECTIVITY COEFFICIENTS OBTAINED FOR THE PULSED
CHRONOPOTENTIOMETRIC POLYMERIC MEMBRANE ION SENSORS**

Hasini Perera, Alexey Shvarev*.

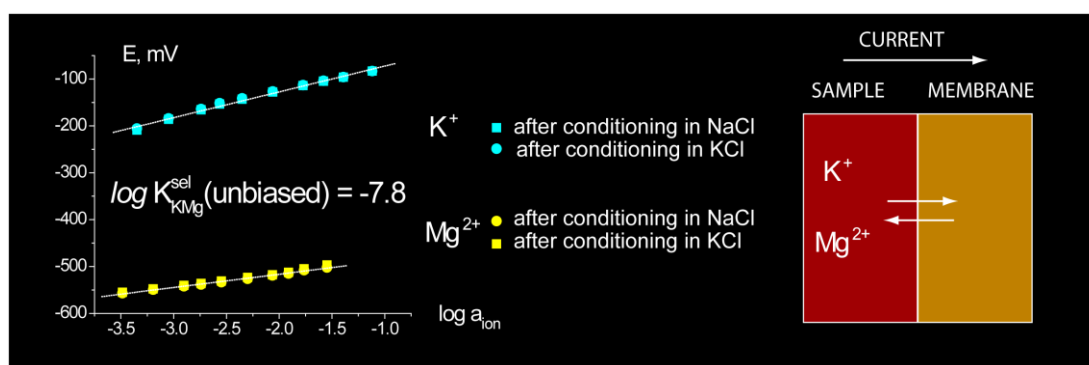
Journal of American Chemical Society

1155, 16th Street N.W., Washington, DC20036

Volume 129(2007), Issue 51, 15754-15755

2.1 Abstract

We report here on the successful observation of the unbiased thermodynamic selectivity of ion-selective sensors working in normal pulse chronopotentiometric mode (pulstrodes). In contrast to ion-selective electrodes the pulstrodes do not require careful counterbalancing the transmembrane ionic fluxes to achieve unbiased thermodynamic selectivity. The pulstrodes can work under asymmetric conditions, which are often encountered in practice. The composition of the inner filling solution did not affect the sensor response indicating that the transmembrane flux of primary ions was indeed effectively suppressed in the absence of ion-exchanger. For the K-selective sensor considered here an improvement of Mg discrimination by factor of 1000 was demonstrated



2.2 Communication

We report here on the successful observation of the unbiased thermodynamic selectivity of galvanostatically controlled ion-selective sensors. In contrast to their potentiometric counterparts the selectivity of the sensors is not affected by the conditioning procedure or composition of inner filling solution. For the K-selective sensor considered here a 1000-fold difference in biased and thermodynamic selectivity was found.

Selectivity is clearly one of the most critical parameters of the ion-selective electrodes (ISEs). Until the past decade, it was a common knowledge that the potentiometric selectivity of ISEs in most cases can not exceed a factor of $10^{-3} - 10^{-4}$. The discovery of the role of trans-membrane fluxes and the fact that leaching of primary ions into the sample biases the selectivity of the sensor^{1,2} revolutionized the field of ISEs.

In the series of experiments described by Bakker^{1,2} the unbiased thermodynamic selectivity was obtained for the ion-selective membranes, which have never been in contact with primary ion before detecting the discriminated ions. Once the membrane was exposed to the primary ion solution, the electrode will no longer respond to the discriminated ions in the Nernstian manner and biased selectivity coefficients were observed. Thus, this approach is of limited practical applicability.

Ideally, the unbiased ISE response can be observed if the composition of the sample and inner filling solution are identical. However, this requirement is hard to fulfill in practice. Any composition misbalance will likely induce a concentration gradient and the corresponding ionic flux in either direction.

A number of research groups have developed measures to eliminate transmembrane diffusion. The first approach was to reduce and stabilize the concentration of primary ions in the inner filling solution using complexing agents such as EDTA.³ This method was limited, however, to the analytes, which can be buffered. Ion exchange resins have also been used in order to maintain a low activity of primary ions in the inner solution.⁴ The lifetime of ISEs with buffered inner filling solution is limited in

presence of steady ionic fluxes toward the inner compartment depending on the flux rate and the ion-exchange or buffer capacity of the internal solution.

Other approaches included the reducing of transmembrane diffusion by lowering the concentration of ion-exchanger⁵, increasing the thickness of the membrane^{6,7}, using the polymer with lower ion diffusion coefficients⁸, and facilitating the diffusion in aqueous sample by stirring.⁴ Use of external current to compensate for bias zero-current flux has been proposed.⁹

Very recently pulsed ion-selective sensors (termed pulstrodes) were introduced, which are based on electrochemically induced periodic ion extraction.¹⁰ A current pulse was applied to the sensor to induce a flux of ions from the sample into the membrane. This method was further modified to set the current to zero after the current pulse and measure the potential eliminating iR drop across the membrane.¹¹ The resulting potential depends on the ion activity ratio at the interface and, thus, obeyed the Nernst and Nikolski-Eisenmann equation and, consequently, the sensor response mimicked the response of potentiometric ISE. In order to strip extracted ions a stripping potential was applied in the potentiostatic mode.

The process of ion extraction was made completely reversible because the ion-exchanger in the membrane was replaced with a lipophilic electrolyte and, thus, the membrane did not possess ion-exchange properties. Several important advantages of this technique over classical potentiometric ISEs were demonstrated including multianalyte detection capability,¹⁰ reversible response to polyionic compounds such as anticoagulant heparin and its antidote protamine,¹² drastic improvement of sensitivity,¹³ and a possibility to simultaneously detect activity and total concentration of a complexed ion in the aqueous sample.¹⁴ The selectivity of the pulstrodes can be improved by kinetic discrimination of the discriminated ion.¹⁵

However, perhaps the most important and significant advantage of galvanostatically controlled ion-selective sensors was overlooked. If the membrane does not contain ion-exchange sites, the spontaneous transmembrane ionic fluxes in either direction are

eliminated regardless of the composition of the sample and inner filling solution. Moreover, the presence of primary ion in the inner filling solution of a pulstrode is not required because the potential at the inner interface under applied current is dictated by the extracted anions.¹⁶ Thus, the sensors can exhibit the selectivity that is not biased by the leaching of primary ions from the membrane.

We fabricated pulsed galvanostatic potassium selective electrodes based on ionophore valinomycin. The membrane of the pulstrodes was doped with lipophilic electrolyte tetradodecylammonium tetrakis(4-chlorophenyl)borate (ETH 500). The inner filling solution contained 10 mM NaCl or KCl.

The pulstrode response is shown in Figure 2.1. The potential was measured in zero current mode (1 s) after 1 s cathodic current pulse of $-25 \mu\text{A}$ was applied.

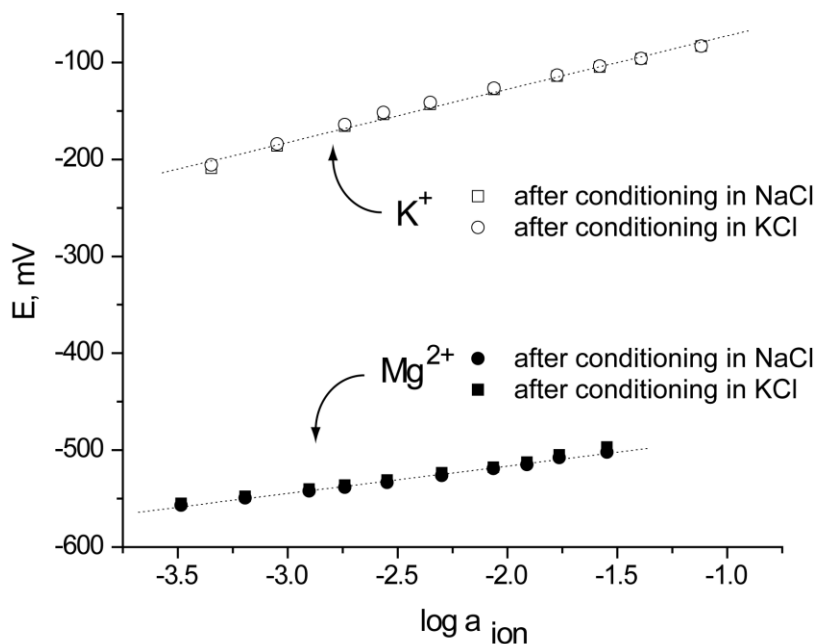


Figure 2.1. Response of K-selective pulstrodes towards chloride salts of K and Mg. The inner filling solution contains A) 0.01 M NaCl, the slopes are 59.3 and 29.0 mV dec⁻¹ B) 0.01 M KCl, the slopes are 61.2 and 27.9 mV dec⁻¹. Electrodes are conditioned with the solution similar in composition to the inner filling solution. The dotted lines are linear fits. The corresponding selectivity coefficient was $\log K_{K,Mg} = -7.8$ regardless to the composition of the conditioning or inner filling solution. The potential was measured in zero current mode (1 s) after 1 s cathodic current pulse of $-25 \mu\text{A}$ was applied.

After conditioning in NaCl (Figure 2.1A) solution, pulsed galvanostatic electrodes showed near Nernstian responses to discriminated ion as well as for the primary ion. The resulting selectivity coefficient calculated according Nikolskii-Eisenmann formalism¹ was $\log K_{K,Mg} = -7.8$. As it can be seen in Figure 2.1B, the overnight conditioning in KCl solution did not cause a significant change in pulstrode response to the primary and discriminated ions. The sensors retained the unbiased thermodynamic selectivity.

It should be noted that the observed discrimination of magnesium is not kinetic¹⁵ because the concentration range used here is higher than the critical ion concentration¹⁴ at which interface concentration depletion occurred.

The composition of the inner filling solution did not affect the sensor response. The use of inner solutions contained 10 mM NaCl and KCl yielded practically the same calibration curves and selectivities. This experimental fact indicated that the transmembrane flux of sodium ions was indeed effectively suppressed in the absence of ion-exchanger.

The response of the pulstrodes was directly compared to the response of K-selective ISEs. The potentiometric ISE membrane was doped with highly lipophilic sodium tetraphenylborate derivative. The conditioning procedure proposed by Bakker¹ was used. The K-selective ISEs, which were conditioned in NaCl solution showed an unbiased selectivity ($\log K_{K,Mg} = -7.0$) and the Nernstian response slopes towards primary and discriminated ions (Figure 2.2A).

After the electrodes were exposed to the solution containing primary ion the resulting ISE response towards Mg shown in Figure 2.2B was heavily masked by the primary ions leaching from the membrane. The slope of Mg calibration curve was only 9.0 mV/dec. As it was demonstrated previously,¹ the transmembrane flux of potassium ions caused dramatic decrease of apparent selectivity by more than 2 orders of magnitude ($\log K_{K,Mg} = -5.4$).

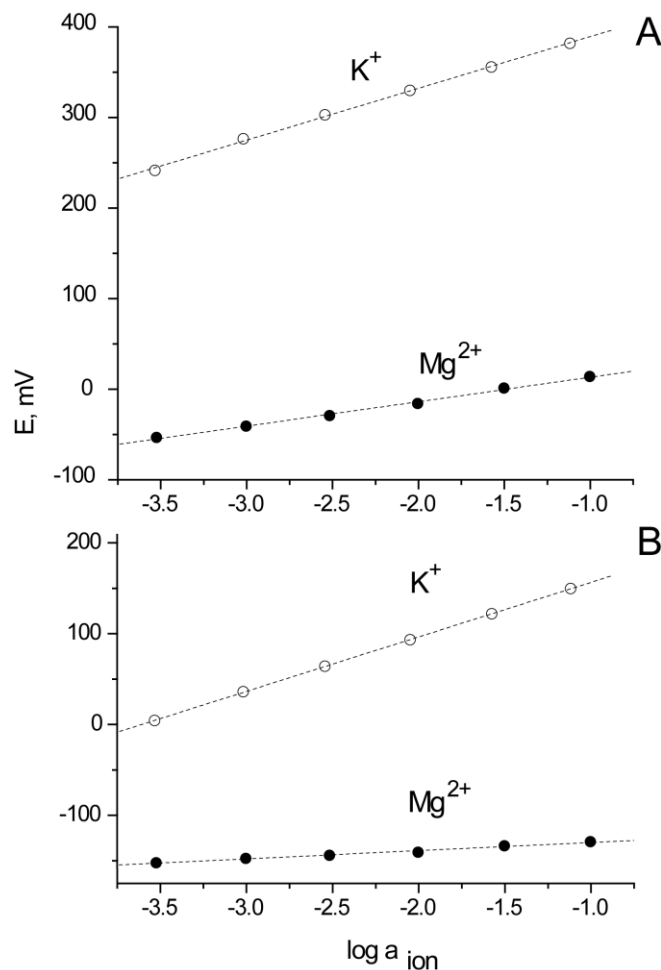


Figure 2.2. Response of K-selective potentiometric electrodes conditioned in A) 0.01 M NaCl. (the response slopes are of 57.2 mV/dec and 27.0 mV/dec) B) 0.01 M KCl towards chloride salts of K and Mg. (the response slopes are of 59.9 mV/dec and 9.0 mV/dec.) The composition of inner filling solution is identical to the composition of the conditioning solution. The dashed lines are linear fits.

In contrast to their potentiometric counterparts, the pulstrodes do not require careful counterbalancing of the transmembrane ionic fluxes and can work under asymmetric conditions, which are often encountered in practice. We believe that this observation is of importance in clinical analysis, where high selectivity of the sensor is especially valuable in presence of a large interfering background, which often is found in the physiological samples such as whole blood or serum.

2.3 Supporting Information

2.3.1 Reagents.

High molecular weight poly(vinyl chloride)(PVC), bis(2-ethylhexyl) sebacate (DOS), valinomycin, tetradodecylammonium tetrakis-(4-chlorophenyl)borate (ETH 500), tetrahydrofuran (THF), and all salts were purchased from Sigma – Aldrich (Milwaukee, WI). Aqueous solutions were prepared by dissolving the appropriate salts in deionized water (18.2 M Ω cm).

2.3.2 Pulsed Galvanostatic Electrodes

Pulsed galvanostatic electrode membrane is contained of Valinomycin 1.1 wt% (9.9 mmol kg⁻¹), tetradodecylammonium tetrakis-(4-chlorophenyl)borate 8.3 wt% (72.3 mmol kg⁻¹), poly(vinyl chloride) 30.2 wt%, bis(2-ethylhexyl) sebacate (DOS) 60.4 wt% totaling 140.65 mg. The constituents were dissolved in ca.1.5 ml of tetrahydrofuran (THF). By casting this solution into a plastic ring of 22 mm diameter, membrane of ca. 200 μ m thicknesses were obtained. The ion-selective membranes were cut with a cork borer (6.6 mm in diameter) from the parent membrane and incorporated into a Philips electrode body (IS-561, Glasbläserei Möller, Zurich, Switzerland) with the Ag/AgCl internal reference electrode. The inner filling solution contained either 0.01M NaCl or 0.01M KCl. The exposed membrane area was 0.08 cm². Electrodes were conditioned overnight in a solution identical to its inner filling solution.

2.3.3 Chronopotentiometric measurements.

A conventional three-electrode cell was used for chronopotentiometric measurements. The membrane electrode was connected as a working electrode. A high surface area platinum wire cage was used as a counter electrode. The reference electrode was a double junction Ag/AgCl electrode with saturated KCl as the inner solution and 1 M LiOAc as a bridge electrolyte.

A modified AFCBP1 bipotentiostat (Pine Instruments, Grove City, MA) controlled by a PCI-6221 data acquisition board and LabVIEW 7.1 software (National Instruments, Austin, TX) on a PC was used for the measurements.¹¹

An uptake current pulse of 1 s was followed by setting current to zero. Sampled potentials were obtained as the average value during the last 10% of this zero current pulse. Thus, the potential values did not contain an iR drop. To expel the extracted ions the stripping potential was applied in potentiostatic mode for 10 s. The background electrolyte was 0.01 M *tris*-HCl buffer solution (pH ca. 8.0).

2.3.4 Potentiometric Electrodes

The ion-selective electrode membranes were cast by dissolving valinomycin 1.19 wt% (10.62 mmol kg⁻¹), Sodium tetrakis[3,5- bis(trifluoromethyl)phenyl]borate 0.56 wt% (6.338 mmol kg⁻¹), Poly(vinyl chloride) 32.77 wt% , and Bis(2-ethylhexyl) sebacate (DOS) 65.48 wt% totaling 140.65 mg in 1.5 ml THF and pouring it into a plastic ring (22 mm id) affixed onto a microscopic glass slide.

For each electrode, a 6.6 mm diameter disk was cut with a cork borer from the parent membrane and incorporated into a Phillips electrode body (IS-561, Glasbläserei Möller, Zurich, Switzerland). Either 0.01 M NaCl or 0.01 M KCl served as the internal filling solution for the assembled electrodes. The electrodes were conditioned in a solution identical to the inner filling solution overnight before measurement.

2.3.5 Potentiometric measurements

All membrane electrode potential measurements were performed at laboratory ambient temperature vs. a double junction Teflon sleeve Ag/AgCl reference electrode (Ingold, Wilmington, MA) in a galvanic cell of the type:

Ag/ AgCl / KCl / 1 M LiOAc //sample // membrane // inner filling solution / AgCl / Ag

Potentials were measured in unstirred solutions via a custom built potentiometric station, which included several electrometric amplifiers (AD820, Analog Devices)

connected to the 24-bit 8-channel data acquisition board NI-4351 controlled by LabVIEW software (National Instruments, Austin, TX) To minimize the noise, final e.m.f. values were calculated as the mean of the individual data points over 60 sec. measurements.

2.4 Acknowledgement.

The authors acknowledge the College of Science and the Department of Chemistry at Oregon State University for financial support of this research.

2.4 References

- (1) Bakker, E. *J. Electrochem. Soc.* **1996**, *143*, L83 - L85.
- (2) Bakker, E. *Anal. Chem.* **1997**, *69*, 1061-1069.
- (3) Sokalski, T.; Ceresa, A.; Zwickl, T.; Pretsch, E. *J. Am. Chem. Soc.* **1997**, *119*, 11347-11348.
- (4) Szigeti, Z.; Vigassy, T.; Bakker, E.; Pretsch, E. *Electroanalysis* **2006**, *18*, 1254 - 1265.
- (5) Ceresa, A.; Bakker, E.; Hattendorf, B.; Gunther, D.; Pretsch, E. *Anal. Chem.* **2001**, *73*, 343-351.
- (6) Sokalski, T.; Zwickl, T.; Bakker, E.; Pretsch, E. *Anal. Chem.* **1999**, *71*, 1204 - 1209.
- (7) Sokalski, T.; Ceresa, A.; Fibbioli, M.; Zwickl, T.; Bakker, E.; Pretsch, E. *Anal. Chem.* **1999**, *71*, 1210 - 1214.
- (8) Qin, Y.; Peper, S.; Radu, A.; Ceresa, A.; Bakker, E. *Anal. Chem.* **2003**, *75*, 3038-3045.
- (9) Lindner, E.; Gyurcsanyi, R. E.; Buck, R. P. *Electroanalysis* **1999**, *11*, 695 - 702.
- (10) Shvarev, A.; Bakker, E. *Anal. Chem.* **2003**, *75*, 4541 - 4550.
- (11) Makarychev-Mikhailov, S.; Shvarev, A.; Bakker, E. *J. Am. Chem. Soc.* **2004**, *126*, 10548-10549.
- (12) Shvarev, A.; Bakker, E. *J. Am. Chem. Soc.* **2003**, *125*, 11192-11193.
- (13) Makarychev-Mikhailov, S.; Shvarev, A.; Bakker, E. *Anal. Chem.* **2006**, *78*, 2744-2751.
- (14) Shvarev, A.; Bakker, E. *Talanta* **2004**, *63*, 195-200.
- (15) Gemene, K. L.; Shvarev, A.; Bakker, E. *Anal. Chim. Acta* **2007**, *583*, 190-196.
- (16) Perera, H.; Fordyce, K., M.; Shvarev, A. *Anal. Chem.* **2007**, *79*, 4564-4573.

CHAPTER 3

**DETERMINATION OF UNBIASED SELECTIVITY COEFFICIENTS USING
PULSED CHRONOPOTENTIOMETRIC POLYMERIC MEMBRANE ION
SENSORS**

Hasini Perera, Alexey Shvarev*

Analytical Chemistry

1155, 16th Street N.W, Washington, DC 20036

Volume 80 (2008), Issue 20, 7870-7875

3.1 Abstract

A new procedure for the determination of selectivity coefficients of neutral carriers using pulsed chronopotentiometric ion selective sensors (pulstrodes) is established. Pulstrode membrane which lacks an ion-exchanger suppresses the zero current ion flux, allowing a Nernstian response slope for even highly discriminated ions. Unlike previously developed methods unbiased selectivity remains unaltered even with the exposure to the primary ion solution for prolonged time. Studies with potassium-, silver-, and calcium-selective electrodes reveal that pulstrodes yield the same or slightly favorable unbiased selectivity coefficients than reported earlier. In contrast to alternative methods for the determination of unbiased selectivity this technique offers a unique simplicity and reliability. Therefore the new procedure promises to be a valuable additional tool for the characterization of unbiased selectivity coefficients for the ISEs.

3.2 Introduction

Until recently carrier-based ion selective electrodes (ISEs) were accepted universally as analytical tools that are used in detecting relatively high concentration of selected ions. The observed low detection limit was attributed to insufficient selectivity of the ISEs. The discovery of transmembrane fluxes and the fact that leaching of primary ions into the sample biases the selectivity of the sensor revolutionized the field of ISEs.^{1,2}

One of the most important consequences of properly understanding the zero current membrane flux was the realization that the unbiased or true thermodynamic selectivity of known ionophores is, indeed, much better than demonstrated previously. Thus, lower detection limit of the ISE can be significantly improved. Laborious studies in several research groups have resulted in significant improvement with the detection limit of silver³, lead⁴, cadmium⁵, and cesium⁶ leading to nanomolar or lower concentrations.

Though tremendous advancements have been reached in detecting various ions over the past decade, there are still major challenges in the area of ISEs. For example, some physiologically important ions such as Li^+ , Mg^{2+} and Cl^- still cannot be detected directly, in complex matrices using the traditional ISEs due to high levels interferences.^{7, 8} The measurement of lithium in blood serum is interfered by high concentration of sodium⁹ and the measurement of magnesium in serum is hindered by calcium.¹⁰ The major challenge for these ISEs is the required high selectivity against the background. Therefore the quest for new and more selective ionophores will continue.

One of the most important tools in this search is a reliable method for the determination of the unbiased selectivity coefficients. It is now known, that most selectivity coefficients reported in the literature were biased due to the zero current ion flux. The differences found between unbiased and biased selectivity coefficients can be up to 6 and 11 orders of magnitude for monovalent and divalent ISEs,¹¹ respectively.

Several publications¹¹ and reviews¹²⁻¹⁴ have covered the various experimental conditions that allow the determination of unbiased selectivity coefficients. Most of these methods require either avoiding exposure to primary ion before measuring the discriminate ion,^{15, 16} careful optimization of the inner filling solution or the sample solution depending on the ion of interest,^{2, 17} optimization of the membrane composition^{4, 18} and thickness^{19, 20} in order to reduce the diffusion layer thickness or application of external current to compensate for zero current flux.²¹ The abovementioned methods are rather complex and require a laborious experimental procedures.

In a recent short communication, we have reported on obtaining unbiased selectivity coefficients using pulsed chronopotentiometric polymeric membrane ion sensors or the pulstrodes²² The application of normal pulse chronopotentiometry to solvent polymeric membrane electrodes was introduced by Bakker and coworkers and is described in detail in a series of previous publications.²³⁻²⁵

As we emphasized in the communication, pulstrode membrane effectively suppress the zero current ion flux without any optimization process unlike its potentiometric counterpart. Thus, the pulstrodes have no apparent “memory effect” always exhibiting unbiased selectivity regardless of the conditioning method.

In this paper, we introduce this novel simple method as a general procedure to characterize the selectivity of carrier-based ion-selective electrodes. The principle of the new procedure, including the general utility of the method is established experimentally with a variety of selective carriers including potassium, silver and calcium described here.

3.3 Experimental Section

3.3.1 Reagents.

High molecular weight poly(vinyl chloride)(PVC), 2-nitrophenyl octyl ether (o-NPOE), dioctylsebacate (DOS), valinomycin (potassium ionophore I), S,S'-Methylene-bis(N,N-diisobutyldithiocarbamate) (MBDiBDTC, marketed as lead ionophore II), calcium ionophore N,N-Dicyclohexyl-N',N'-dioctadecyl-3-oxapentanediamide (ETH 5234), tetradodecylammonium tetrakis-(4-chlorophenyl)borate (ETH 500), tetrahydrofuran (THF), and all salts were purchased from Sigma – Aldrich (Milwaukee, WI). All other chemicals were purchased from VWR (West Chester, PA). Aqueous solutions were prepared by dissolving the appropriate salts in deionized water (18.2 MΩ cm).

3.3.2 Membrane Preparation.

The membrane matrices contained the carrier and ETH500 together with polymer (PVC) and plasticizer (1:2 by weight) to give a total cocktail mass of 140 mg. Dioctylsebacate was used for potassium-selective membranes, and calcium and silver-selective membranes were prepared with o-NPOE. Potassium-selective membranes

contained 10 mmol kg⁻¹ potassium ionophore and 44 mmol kg⁻¹ of the lipophilic salt ETH 500. Calcium and silver selective membranes contained 14 mmol kg⁻¹ of respective ionophore and 72 mmol kg⁻¹ of the lipophilic salt ETH 500. The membrane films (~200 μm thick) were fabricated by solvent casting with THF as a solvent.

3.3.3 Liquid-contact electrodes.

The ion-selective membranes were cut with a cork bore (6.6 mm in diameter) from the parent membrane and incorporated into the Philips electrode body (IS-561, Glasbläserei Möller, Zurich, Switzerland) with the Ag/AgCl internal reference electrode. The exposed membrane area was 0.08 cm². Calcium and potassium-selective pulstrodes were filled with 0.01 M NaCl. The solution of 0.01 M NaNO₃ was used as an inner filling solution for silver-selective pulstrodes. The electrodes were conditioned overnight in the solutions with the composition which was identical to the composition of the inner filling solutions.

3.3.4 Chronopotentiometric measurements.

A conventional three-electrode cell was used for chronopotentiometric measurements. The membrane electrode was connected as a working electrode. A high surface area coiled platinum wire was used as a counter electrode. The reference electrode was a double junction Ag/AgCl electrode with saturated KCl as the inner solution and 1 M LiOAc as a bridge electrolyte.

A modified²²AFCBP1 bipotentiostat (Pine Instruments, Grove City, MA) controlled by a PCI-6221 data acquisition board and Lab View 7.1 software (National Instruments, Austin, TX) on a PC was used for measurements.

It should be noted that the main purpose for the modification was fast switching between potentiostatic and galvanostatic modes. Although most of commercially available instruments do not contain this feature, such a modification is relatively simple and inexpensive. The modification can be done in several different ways, for example, connection the PC-controlled solid-state relay to the “mode” tumbler. For the

bipotentiostat the solid state relay switches the membrane electrode between two WE outputs, one of which works in galvanostatic and the second one in the potentiostatic mode.

Triple pulse mode²³ was used in which a 1 s current pulse is followed by a zero current measurement pulse and a 10 s potential controlled baseline potential pulse. Potentials were obtained as the average value during the last 10% of each 1 s uptake pulse (applied current mode/galvanostatic mode) and of each zero current pulse (zero current mode/potentiostatic mode). All of the data presented here are obtained during zero current pulse measurements.

All experiments were conducted at ambient temperature (23 ± 2 °C). Activity coefficients were calculated according to Debye-Hückel formalism.²⁴

3.4 Results & Discussion

A schematic representation of the expected concentration profiles in the membrane of the ISE is shown in Figure 3.1A. Assume that the polymeric ISE membrane separates aqueous sample and inner filling solution and both solutions contain the same electrolyte I^+X^- . The membrane is doped with lipophilic ion-exchanger R^- , and the ionophore, which forms a lipophilic complex $[IL]^+$ with the primary ion I^+ . There $a_i(\text{aq, pb})$, $a_i(\text{org, pb})$, and $a_i(\text{aq, ifs})$ refer to the activities of species i at the interface in aqueous, membrane, and inner filling solution phases, respectively.

The role of transmembrane ion-flux is insignificant if the concentration of the target species is above 1 μM . However, at low activities of the analytes, the transmembrane ion flux causes an elevated concentration of primary ions in the vicinity of the membrane (Figure 3.1A). This causes a strong bias of the resulting apparent selectivity. The response to the discriminated ions in most cases is strongly sub-Nernstian.

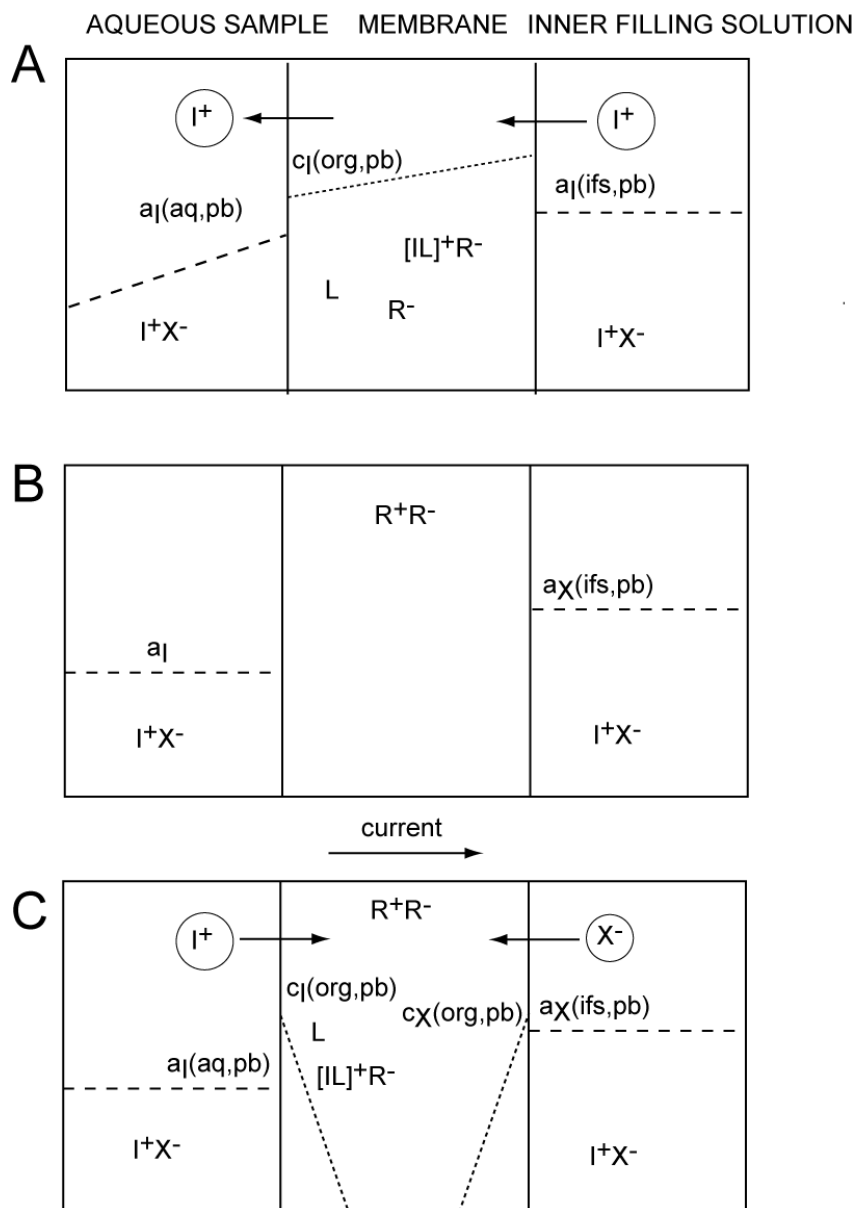


Figure 3.1. Schematic representation of concentration gradients of the primary ions in (A) traditional potentiometric ISE. (B) The pulstrade in its potentiostatic working mode. (C) The pulstrade in the galvanostatic working mode. In this mode a defined cationic flux is generated towards the membrane.

One important goal of this work is to demonstrate that, if the ISE membrane is under galvanostatic control, even the highly discriminated ions produce Nernstian slope and unbiased selectivity regardless of the experimental conditions.

In contrast to its potentiometric counterpart the polymeric membrane of the pulstrode contains an ionophore L and inert lipophilic salt (R^+R^-) in the polymer matrix (Figure 3.1B). In absence of ion exchanger the spontaneous extraction of the primary ion to the membrane is effectively suppressed.

A current pulse imposed across the membrane causes the extraction of ions into the membrane (Figure 3.1C). As established in previous work, potential across the membrane in galvanostatic mode is the sum of phase boundary potentials at both sides of the membrane and Ohmic potential drop across the membrane.²⁸ Further considering that primary ions extracted in to the membrane could be in either their uncomplexed or complexed form of fixed stoichiometry²² potential across the membrane (E_m) in galvanostatic mode can be expressed using the following equation:

$$E_m = \frac{RT}{z_I F} \ln a_{I(aq,pb)} + \frac{RT}{z_X F} \ln a_{X(ifs,pb)} + \frac{RT}{z_I F} \ln \frac{1}{c_{ILn(org,pb)}} + \frac{RT}{z_I F} \ln \frac{k_I FA \sqrt{D_{org}}}{2i\sqrt{t}} + \frac{RT}{z_X F} \ln \frac{k_X FA \sqrt{D_{org}}}{2i\sqrt{t}} + iR$$

where k_I is the free energy of transfer for an ion I, $a_{I(aq/ifs, pb)}$ are the phase boundary activities of species i in the aqueous contacting phase, i is the applied current, R_m is the membrane resistance, t is the duration of the pulse, A is the membrane area, D_{org} is the diffusion coefficient in the membrane phase, $c_{ILn(org,pb)}$ is the concentration of primary ion-ionophore complex in the membrane and R , T and F have their usual meanings.

According to the equation, the membrane potential of the pulstrode under applied current depends on the amplitude and the duration of the current pulse, the concentration of the complexed primary ion-ionophore, and the activities of ions in the sample solution and counter ions in the inner filling solution.

The galvanostatic pulse is followed by the switching to the potentiostatic mode. During this time period all extracted ions will be released to the solution to satisfy the phase boundary conditions of the membrane.

Assuming that all ions extracted into the membrane are released in the potentiostatic mode and if the current, pulse duration, and the composition of inner filling solution are constant, the last five terms of the equation become constant. The resulting response is described by the first term, which is the Nernst equation, and the potential across the membrane reduces to:

$$E_m = \frac{RT}{z_I F} \ln a_{I(aq, pb)}$$

The Nernstian slope is obtained irrespective of the amplitude or the magnitude of the applied current.

Recently in a short communication, we reported on obtaining Nernstian slope for a highly discriminated ion Mg^{2+} on a valinomycin based K^+ selective pulstrode yielding the same unbiased selectivity coefficients reported for the carrier.²¹ Even though unbiased selectivity was observed using the potentiometric electrodes, once the membrane was exposed to a primary ion solution, electrode no longer responded to the discriminated ion in Nernstian manner.^{15, 16} Further, precautions have to be taken while preparing the membrane and testing to avoid contact with the primary ion. Moreover only limited test time was available after the introduction of the primary ion, as long-term drifts were expected due to the change in the membrane composition.^{15, 16}

We were successful in obtaining unbiased selectivity regardless of whether pulstrodes were exposed to its primary ions. As this was outlined above, the Nernstian slope for discriminated ions are observed since zero current ion flux is eliminated in the pulstrode membrane. Here, we are establishing the method to be generally useful by critically evaluating it with number of widely used neutral carriers. Valinomycin, ETH 5234 an established calcium ionophore, and a very selective Ag carrier MBDiBDTC

are evaluated in the study. We compared the selectivity of the pulstrodes with the selectivities reported earlier, which were obtained by the method developed by Bakker.^{15,16}

It was established earlier, the conditioning solutions has no effect on the selectivity coefficients determined using pulstrodes.²¹Therefore further studies were not carried out to strengthen this claim. However, the primary ions present in the conditioning solution represent a source of contamination. Extremely high selectivity coefficients measured in this work require additional precautions such as using only polypropylene lab ware and multiple washing steps with deionized water to avoid possible contamination. Further if not specified otherwise, the pulstrodes tested here were conditioned in discriminating ion solution to minimize the possibility of any errors.

Valinomycin pulstrodes were studied with respect to a variety of discriminating ions. In Figure 3.2, the response of valinomycin based pulstrodes towards various electrolytes are shown. All highly discriminating ions show a near-Nernstian response slope. As shown on the diagram in Fig. 3, the selectivity coefficients obtained with the pulstrodes are in good agreement with the published values, thus confirming that use of pulstrode is a valid method for the determination of unbiased selectivity coefficients. We even observed a slight improvement of the selectivity with the pulstrodes over previously reported results, which can be attributed to the extreme sensitivity of potentiometric sensors to the primary ion impurities.

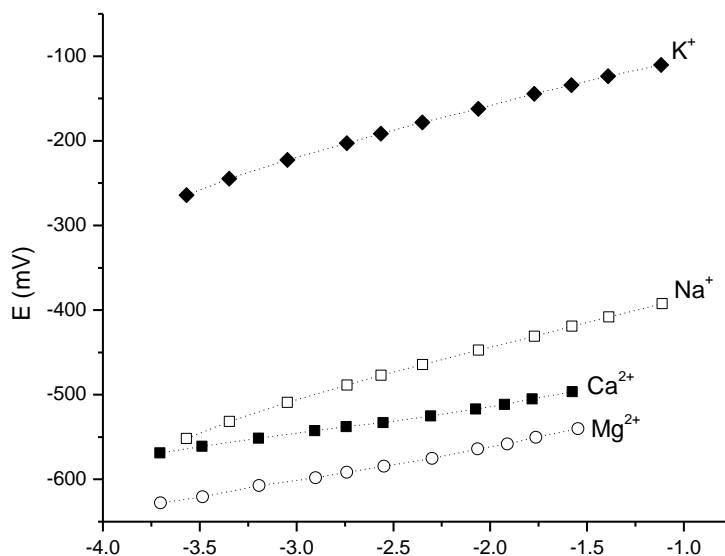


Figure 3.2. Response of K-selective pulstrodes towards chloride salts of K^+ (slope 60.0 mV/dec), Na^+ (slope 59.8 mV/dec), Ca^{2+} (slope 33 mV/dec) & Mg^{2+} (slope 40.3 mV/dec) Electrodes are conditioned and filled with 0.01 M NaCl. Potential measured zero current mode with 0.01 M TRIS (pH=7) as a background electrolyte.

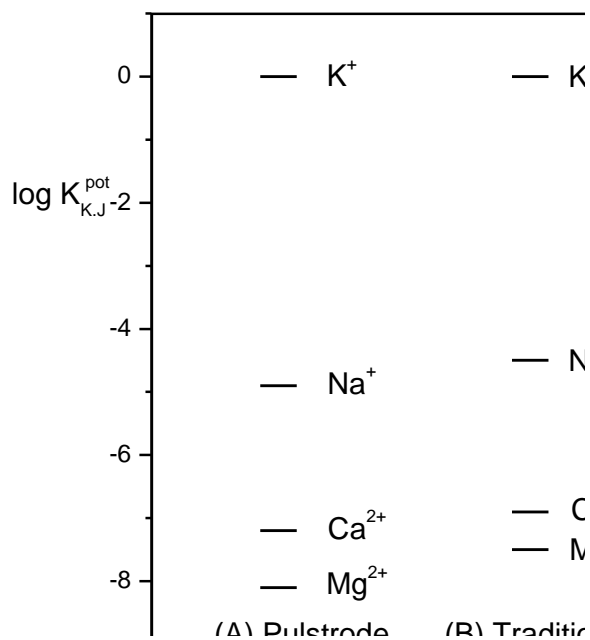


Figure 3.3. Experimental selectivity coefficients, ($\log K_{K,J}^{pot}$) for (A) K-selective PVC-o-NPOE (1:2) pulstrode membranes containing valinomycin and ETH 500 (B) K-selective PVC-DOS (1:2) potentiometric membranes containing valinomycin and Sodium tetrakis[3,5-bis(trifluoromethyl)phenyl] borate. (NaTFPB)¹⁵

It is well-known that monovalent cation selectivity is improved with the use of a non polar/less polar plasticizer. We faced problems in long-term stability of the pulstrode membrane when dioctylsebacate (DOS) was used as the plasticizer due to apparent incompatibility with the high concentration of the lipophilic salt ETH500. Specifically, we observed slow crystallization of ETH500 in the membrane phase. In order to stabilize the membrane composition, we reduced the concentration of the ETH500 from 72 to 44 mmol/kg. This problem may also be overcome using more lipophilic inert electrolytes, for example, by replacing tetrakis-(4-chlorophenyl)borate with tetrakis[3,5-bis(trifluoromethyl)phenyl] borate in the ETH500. Silver and calcium-selective membranes contained *o*-NPOE as the plasticizer and there was no sign of the ETH500 crystallization over a period longer than a month.

In figure 3.4, an analogous experiment is shown with a highly selective silver carrier, MBDiBDTC. Even though Nernstian response is observed for silver at low activities, a slope with a reversal sign is observed at high activities. A similar effect has been observed earlier, for potentiometric membranes with highly preferred ions due to the coextraction.¹¹ As a consequence of too strong complexes, the membrane loses its permselectivity and the preferred ion is extracted in to the membrane with the counter ion causing the anion response.

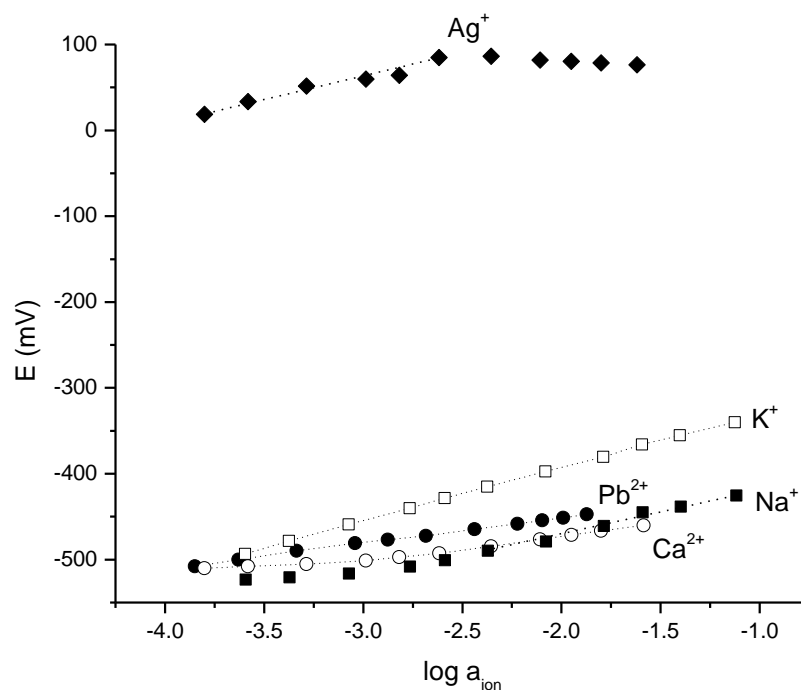


Figure 3.4. Response of Ag-selective pulstrodes towards nitrate salts of Ag⁺ (slope 50.4 mV/dec), Pb²⁺ (slope 29.9 mV/dec), and chloride salts of K⁺ (slope 62.7 mV/dec), Na⁺ (slope 61.8 mV/dec), and Ca²⁺ (slope 29.8 mV/dec). Electrodes were conditioned and filled with 0.01 M NaNO₃. Potential measured in zero current mode with 0.01 M TRIS (pH=7) as a background electrolyte.

Interestingly, this effect is only observed while taking the potential measurement in zero current mode only. Under applied current (data not shown) the sensors demonstrated cationic function even at high activities of the primary ion. One of the possible explanations is that the applied current pulse repels the anions from the membrane. During the zero current mode, however, the coextraction process takes place, which is driven by passive diffusion transport. Owing to its strong complexation, Ag is extracted together with its counter ion. Therefore the selectivity coefficients shown in figure 3.5 are calculated from the Nernstian portion of the response curve obtained at lower activities. Slight improvement of the selectivity coefficients are observed here as well with respect to previously reported results.

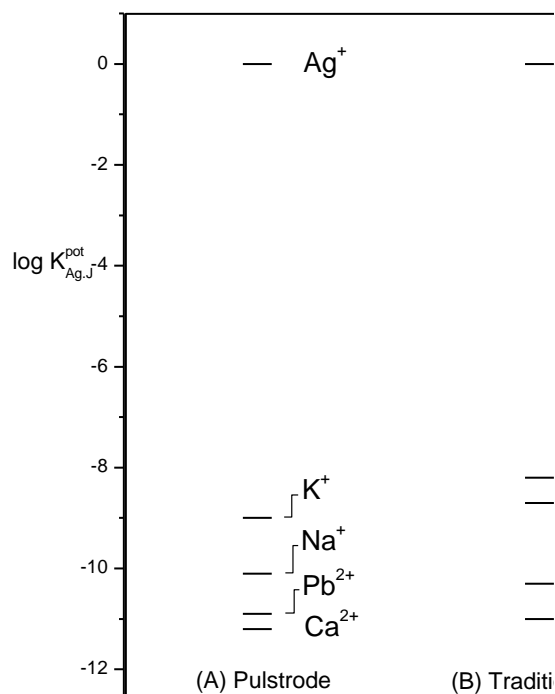


Figure 3.5. Experimental selectivity coefficients, ($\log K_{Ag,J}^{pot}$) for (A) Ag-selective PVC-oNPOE (1:2) pulstrode membranes containing MBDiBTC and ETH 500 (B) Ag-selective PVC-DOS (1:2) potentiometric membranes containing MBDiBDTC and NaTFPB.¹⁶

Ca ionophore (ETH 5234) was first introduced by and Simon and coworkers²⁵. This is very lipophilic ionophore, which is similar in terms of selectivity to well established Ca ionophore ETH 129. The unbiased selectivity coefficients were determined by the buffering of the inner filling solution with a complexing agent.^{17, 19, 20} Moreover it has been found that reduction in the Ca^{2+}/Na^{+} (discriminated ion) activity ratio in the inner filling solution to a certain extent gradually improves both slope and the selectivity. (see Figure 3.6)¹⁸

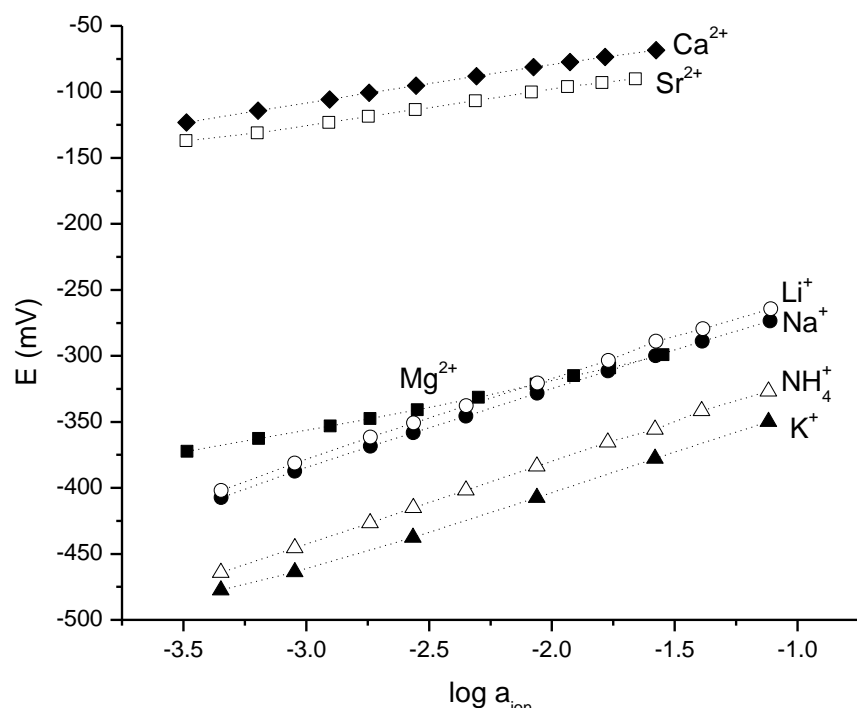


Figure 3.6. Response of Ca-selective pulstrodes towards chloride salts of Ca^{2+} (slope 29.5 mV/dec), Sr^{2+} (slope 27.2 mV/dec), Mg^{2+} (slope 36.5 mV/dec), Li^{+} (slope 61.6 mV/dec), Na^{+} (slope 60.5 mV/dec), NH_4^{+} (slope 61.7 mV/dec) & K^{+} (slope 59.3 mV/dec) Electrodes are conditioned and filled with 0.01 M NaCl. Potential measured in potentiostatic mode with 0.01 M TRIS (pH=7) as background electrolyte.

The optimum selectivity coefficients obtained via tailoring of the internal solution are compared with the pulstrode data. As shown in figure 3.7, the selectivity coefficients for Sr^{2+} , Na^{+} and Mg^{2+} are reasonably close to the previously reported values. Further, more favorable selectivity was observed for Li^{+} , NH_4^{+} and K^{+} with the pulstrodes. The improvement in selectivity could be attributed to complete elimination of transmembrane ion fluxes in the pulstrodes.

Flux of primary ions into the test solution can also be eliminated by the use of solid contact electrodes.²⁶ Selectivity coefficients obtained for NH_4^{+} and K^{+} using pulstrodes agree well with the values obtained with the solid contact ISEs. However, selectivity

coefficients obtained for Li^+ , Na^+ and Mg^{2+} were an order of magnitude higher than those reported for the solid state electrodes.

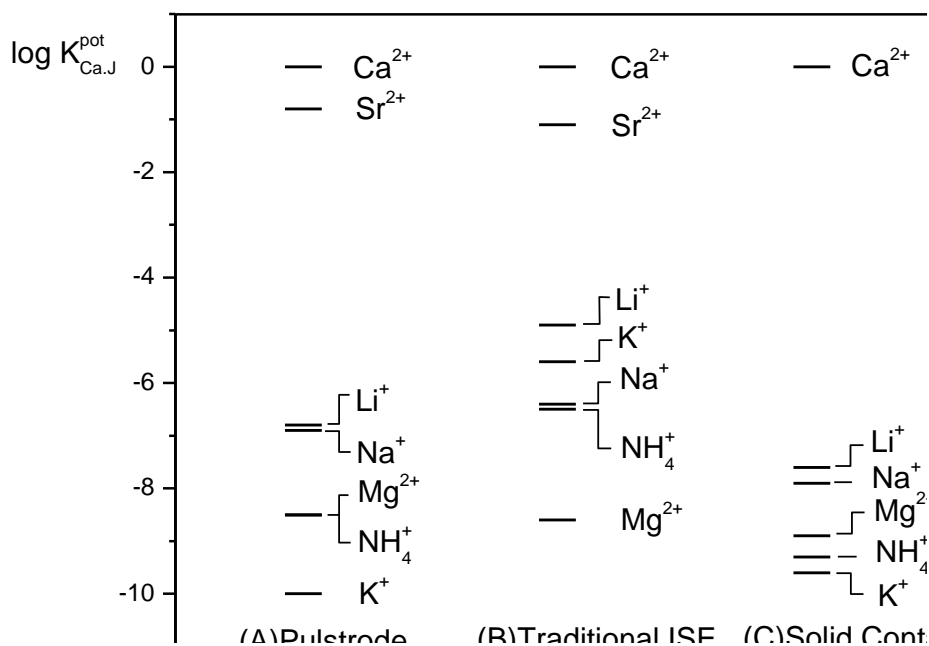


Figure 3.7. Experimental selectivity coefficients, ($\log K_{Ca,J}^{pot}$) for (A)Ca-selective PVC-oNPOE (1:2) pulstrode membranes containing MBDiBTC and ETH 500 (B)Ca-selective PVC-DOS (1:2) potentiometric membranes containing MBDiBDTC and NaTFPB¹⁹ (C) Ca-selective PVC-DOS (1:2) potentiometric solid contact membrane electrodes containing MBDiBDTC and NaTFPB³⁰

The absence of ion-exchanger in the membrane is essential for the response mechanism of a pulstrode. The presence of such impurities, in principle, may be responsible for the small uptake of primary ions and, therefore, for the incomplete stripping. Ionic impurities in solvent polymeric membranes have been known to cause functional potentiometric response in the early ion-selective electrodes (ISEs) without added ion exchanger. The concentration of anionic impurities in a commercially available high purity PVC was found to be on the order of $100 \mu\text{M}/\text{kg}$ ²⁷.

The applied current pulse results in a much higher concentration of primary ions in the membrane at the phase boundary.²² The concentration is on the order of 5 mmol/kg and, thus, the presence of additional ion-exchange impurities can be neglected. This may explain the experimental fact that we did not observe the effects, which can be attributed to the impurities in PVC. However, at very small current densities, the response function and the selectivity of the pulstrode are deteriorated.²² This may be a direct indication that at smaller current densities the ionic impurities rather dictate the phase boundary potential.

One of the possible limitations of this method in the form presented here is its applicability only to the neutral ion carriers. Indeed, a charged ionophore in the membrane matrix will not allow one to reversibly extract ions from the sample. Instead, under applied current, ions will continuously flow across the membrane without forming the concentration gradient and the phase boundary. This limitation can be possibly eliminated by using the ion pair of the charged ionophore with a lipophilic counterion. This will require an additional modification of the ionophore via metathesis with a lipophilic electrolyte, for example, tetradodecylammonium chloride as the countercation or tetrakis-(4-chlorophenyl)borate as the counteranion source. In fact, dinonylnaphthalene sulfonic acid, a lipophilic protamine-selective ionophore, was modified in the same way in order to fabricate a polyion-selective pulstrode.²⁴

3.5 Conclusions

In this paper, unbiased selectivity of three different neutral ion carriers was characterized using galvanostatic control of the polymeric membrane electrodes. The main advantage of this method is its relative simplicity and reliability. There is no need in careful optimization of the experimental conditions depending on the ion of interest.

A major advantage of a pulstrode over the traditional ISEs is the insensitivity towards exposure to the solution containing primary ion. Unlike its potentiometric counterpart,

the pulstrode responds in a Nernstian manner to highly discriminated ions, even after the sensor was exposed to the primary ion. We believe that the transmembrane ionic flux in the pulstrode is completely suppressed. Therefore, the pulstrode operates under experimental conditions, which are ideal for the determination of unbiased selectivity.

The selectivity coefficients reported here are in good agreement with the results previously reported for the potentiometric counterparts. In cases where the counterbalancing of the transmembrane flux with ionic buffers was previously used, selectivity coefficients found for several ions were better than the reported values, confirming that zero current ion flux is minimal in the pulstrodes.

3.6 Acknowledgment

The authors acknowledge the College of Science and the Department of Chemistry at Oregon State University for financial support of this research.

3.7 References

- (1) Bakker, E. P., *E. Anal Chem* 2002, 74, 420A-426A.
- (2) Sokalski, T.; Ceresa, A.; Zwickl, T.; Pretsch, E. *J. Am. Chem. Soc.* 1997, 119, 11347-11348.
- (3) Ceresa, A.; Radu, A.; Peper, S.; Bakker, E.; Pretsch, E. *Analytical Chemistry* 2002, 74, 4027-4036.
- (4) Ceresa, A.; Bakker, E.; Hattendorf, B.; Guenther, D.; Pretsch, E. *Analytical Chemistry* 2001, 73, 343-351.
- (5) Ion, A. C.; Bakker, E.; Pretsch, E. *Analytica Chimica Acta* 2001, 440, 71-79.
- (6) Radu, A.; Peper, S.; Gonczy, C.; Runde, W.; Diamond, D. *Electroanalysis* 2006, 18, 1379 - 1388.
- (7) Lewenstam, A. *Scandinavian Journal of Clinical and Laboratory Investigation, Supplement* 1994, 54, 11-19.
- (8) Lewenstam, A. *Analytical Proceedings* 1991, 28, 106-109.
- (9) Christian, G. D. *Sensors* 2002, 2, 432-435.
- (10) Ben Rayana, M. C.; Burnett, R. W.; Covington, A. K.; D'Orazio, P.; Fogh-Andersen, N.; Jacobs, E.; Kulpmann, W. R.; Kuwa, K.; Larsson, L.; Lewenstam, A.; Maas, A. H. J.; Mager, G.; Naskalski, J. W.; Okorodudu, A. O.; Ritter, C.; St. John, A. *Clinical Chemistry and Laboratory Medicine* 2008, 46, 21-26.
- (11) Bakker, E.; Pretsch, E.; Buehlmann, P. *Analytical Chemistry* 2000, 72, 1127-1133.
- (12) Bakker, E.; Buehlmann, P.; Pretsch, E. *Electroanalysis* 1999, 11, 915 - 933.
- (13) Bakker, E. *Angew. Chem. Int. Ed.* 2007, 46, 5660-5668.
- (14) Bakker, E.; Buehlmann, P.; Pretsch, E. *Chem. Rev.* 1997, 97, 3083 - 3132.
- (15) Bakker, E. *J. Electrochem. Soc.* 1996, 143, L83 - L85.
- (16) Bakker, E. *Anal. Chem.* 1997, 69, 1061-1069.
- (17) Szigeti, Z.; Vigassy, T.; Bakker, E.; Pretsch, E. *Electroanalysis* 2006, 18, 1254 - 1265.
- (18) Sokalski, T.; Ceresa, A.; Fibbioli, M.; Zwickl, T.; Bakker, E.; Pretsch, E. *Anal. Chem.* 1999, 71, 1210 - 1214.
- (19) Sokalski, T.; Zwickl, T.; Bakker, E.; Pretsch, E. *Anal. Chem.* 1999, 71, 1204 - 1209.
- (20) Lindner, E.; Gyurcsanyi, R. E.; Buck, R. P. *Electroanalysis* 1999, 11, 695 - 702.
- (21) Perera, H.; Shvarev, A. *Journal of the American Chemical Society* 2007, 129, 15754-15755.
- (22) Shvarev, A.; Bakker, E. *Anal. Chem.* 2003, 75, 4541-4550.

- (23) Makarychev-Mikhailov, S., Shvarev, A., Bakker, E. *Journal of the American Chemical Society* 2004, *126*, 10548 - 10549.
- (24) Meier, P. C. *Anal. Chim. Acta* 1982, *136*, 363.
- (25) Gehrig, H. R., B. ; Simon, W. *Chimia* 1989, *43*, 377-379.
- (26) Michalska, A. M., K. *Journal of Electroanalytical Chemistry* 2005, *576*, 339-352.
- (27) Qin, Y.; Bakker, E. *Anal. Chem.* **2001**, *73*, 4262–4267.
- (28) Perera, H.; Fordyce, K.; Shvarev, A. *Anal. Chem.* **2007**, *79*, 4564–4573.

CHAPTER 4

CHARACTERIZATION OF [12]-MERCURACARBORAND-4: AN IONOPHORE WITH IODIDE COMPLEXING CAVITY

Hasini Perera, Alexey Shvarev

4.1 Abstract

Highly sensitive and selective iodide electrodes and pulsed chronopotentiometric sensors (pulstrodes) are successfully fabricated using [12]-Mercuracarborand-4 (MC4), a ring reduction equivalent of chloride ionophore, [9]-Mercuracarborand-3 (MC3). Initial studies with MC3 revealed that the pulstrodes are capable in determining unbiased selectivity of neutral anion carriers. Unbiased selectivity coefficients, $\log K_{I,J}^{pot}$, for the principle discriminated ions (J = SCN⁻, Br⁻, NO₃⁻, ClO₄⁻, Cl⁻, OH⁻) were determined to be -3.62±0.11, -5.27±0.03, -5.55±0.28, -6.71±0.07, -6.91±0.42, -9.04±0.53 respectively, which may indicate MC4 as the most selective I⁻ carrier known to date. Potentiometric binding experiments were used to characterize the stoichiometry and the complex formation constant of the ionophore. This revealed the possibility of the formation of extremely stable ($\log \beta_2 = 16.58 \pm 0.28$) [(MC4)₂Cl]⁻ and relatively less stable ($\log K_1 = 5.33 \pm 0.05$) [MC4Cl]⁻.

4.2 Introduction

Carrier based ion selective electrodes have been established as well-known analytical tools used in the determination of cations, in virtually any laboratory. Unfortunately the same can not be said in regard of the anion selective sensors. Most difficulty in the development of anion selective sensors lies in obtaining adequate ionophores that exhibit strong, selective and reversible interactions with anions. In recent years anion complexation by multidentate lewis acid hosts such as mercuracarborands have attracted attention due to their ability to recognize, reversibly bind complementary anions.

Neutral preorganized macrocyclic Lewis acid [9]-mercuracarborand-3 (MC3) (Figure 4.1) was employed as a highly selective ionophore, with the successful fabrication of chloride electrodes and optodes by Bachas *et al.*¹⁻³ Electrodes demonstrated high selectivity for chloride over other anions and the selectivity coefficients obtained were

shown to meet the requirements for clinical applications.¹ Based on the same ionophore optodes confirmed the enhanced selectivity towards chloride and were fully functional over a wide dynamic range with fast response and recovery times.² The MC3 has been studied further by Bakker *et al* as an ionophore for chloride and iodide responsive sensors.⁴⁻⁹ Research carried out in his group has resulted in iodide selective electrodes with nanomolar detection limits⁵ and bulk optodes with ultra-low detection limits in the picomolar range.⁹

Hawthorne and co-workers who originally synthesized MC3, have reported on observation of template effect by halides, in formation of mercuracarborand cycles.¹⁰ In the presence of halides, formation of tetrameric cyclic host, [12]-mercuracarborand-4 (MC4) was observed in place of the less angle strained MC3. Further experiments on MC4-(halide ion) complex has revealed that Hg-halide distances are much shorter indicating strong anion-metal interactions¹⁰. These observations lead us to believe that MC4 have the potential of becoming a halide ionophore resembling its smaller counterpart MC3.

(1)

(2)

Figure 4.1: Chemical structure of Mercuracarborand ionophores
(1) [9]-mercuracarborand-3 (MC3) (2) [12]-mercuracarborand-4 (MC4)

In this paper we investigate MC4 as an ionophore for the development of liquid polymeric electrodes and pulstrodes for iodide. Knowledge of binding information is important for an ionophore in order to design sensors with optimal characteristics. Segmented sandwich membrane method¹¹⁻¹³ was used to determine and compare the complex formation constant of the ionophores MC3 and MC4 with chloride.

Recently, we introduced galvanostatically controlled ISEs with polymeric membranes termed pulstrodes as versatile tools for the determination of unbiased selectivity^{14, 15}. So far all systematic investigations on unbiased selectivity were performed on neutral cation carriers. One objective of this paper is to investigate the capability of pulstrodes to obtain the unbiased selectivity of anion carriers. Selectivity of the MC3 ionophore is determined with the use of pulstrodes as well. Optical sensors made using the same ionophore and the published values for MC3 are used to establish the accuracy of the obtained selectivity.

4.3 Experimental

4.3.1 Reagents.

High molecular weight poly(vinyl chloride)(PVC), plasticizers 2-nitrophenyl octyl ether (o-NPOE) and bis(2-ethylhexyl)sebacate (DOS), lipophilic anion-exchange salts tetradodecylammonium chloride (TDACl) and tridodecylmethylammonium chloride (TDMACl), inert lipophilic salt tetradodecylammonium tetrakis-(4-chlorophenyl) borate (ETH 500), chromoionophore 9-dimethylamino-5-[4-(15-butyl-1,13-dioxo-2,14-dioxanonadecyl)phenylimino]benzo[a]phenoxazine (ETH 5418), a reference dye – 1,1'-dioctadecyl-3,3,3',3'-tetramethylindocarbocyanine perchlorate (DiIC₁₈), tetrahydrofuran (THF), and all salts were purchased from Sigma – Aldrich (Milwaukee, WI). All other chemicals were purchased from VWR (West Chester, PA). Pacific Northwest National Laboratory (Richland, WA) courteously provided the samples of MC3 and MC4. Aqueous solutions were prepared by dissolving the appropriate salts in deionized water (18.2 MΩ cm).

4.3.2 Ion Selective Membrane Preparation.

The electrode membranes were prepared from a component mixture totaling 140 mg. The PVC : plasticizer ratio was 1:2. Only potentiometric ion selective membranes contained DOS as the plasticizer. The component concentrations of the MC3 or MC4 in the pulstrode membranes were 72 mmol/kg ETH500, and 15 mmol/kg MC3 or 10 mmol/kg MC4. Potentiometric MC3 or MC4 membranes contained 15 mmol/kg MC3 or 10 mmol/kg MC4 and 7 mmol/kg TDMACl. The membrane films (~200 μm thick) were fabricated by solvent casting with ~1.5 mL THF as a solvent.

4.3.3 Liquid-contact electrodes.

The ion-selective membranes were cut with a cork bore (6.6 mm in diameter) from the parent membrane and incorporated into a Philips electrode body (IS-561, Glasbläserei Möller, Zurich, Switzerland) with the Ag/AgCl internal reference electrode. The inner filling solution contained 0.01M NaCl. If not stated otherwise, membranes were conditioned overnight in a solution similar to inner filling solution. The exposed membrane area was 0.08 cm^2 .

4.3.4 Chronopotentiometric measurements.

A conventional three-electrode cell was used for chronopotentiometric measurements. The membrane electrode was connected as a working electrode. A high surface area coiled platinum wire was used as a counter electrode. The reference electrode was a double junction Ag/AgCl electrode with saturated KCl as the inner solution and 1 M LiOAc as a bridge electrolyte.

A modified AFCBP1 bipotentiostat (Pine Instruments, Grove City, MA) controlled by a PCI-6221 data acquisition board and LabView 7.1 software (National Instruments, Austin, TX) on a PC was used for measurements¹⁶. An uptake current pulse of 1 s was followed by a zero current measurement pulse and a stripping potential pulse for 10 s. Sampled potentials were obtained as the average value during the last 10% of each 1 s

uptake pulse (applied current mode) and last 10% of the zero current pulse (zero current mode)¹⁷.

4.3.5 Potentiometric Measurements

The potentiometric measurements were recorded with respect to a Ag/AgCl reference electrode using custom built potentiometric station, which included several electrometric amplifiers (AD820, Analog Devices) connected to the 24-bit 8-channel data acquisition board NI-4351 controlled by the LabView software.

Activity coefficients were calculated according to Debye-Hückel formalism¹⁸.

Potentiometric selectivity coefficients (K_{IJ}) were found using separate solution method and the general equation used to calculate the experimental data are given as²¹:

$$\log K_{IJ}^{pot} = \frac{z_I F (E_J - E_I)}{2.303 RT} + \log \left(\frac{a_I}{a_J^{z_I/z_J}} \right) \quad (1)$$

4.3.6 Optode Film Preparation.

Optode films were prepared from a component mixture totaling 90 mg dissolved in 2 mL of THF. PVC:DOS ratio was maintained at 1:2. Optode membranes contained 10 mmol/kg MC3 or MC4, 10 mmol/kg chromoionophore ETH 5418 and 0.1 mmol/kg DiC₁₈.

Thin films were prepared by depositing 50 μ L of cocktail on square, silanized microscope cover slips (22mm wide). The films were left in the air until THF was fully evaporated (30 min). Copverslips were conditioned in MOPS (pH 7.4) buffer for 30 min to activate them.

4.3.7 Sample Preparation for Optical Measurements.

The response curves for anions were measured at a fixed anion concentration (for MC3: Γ 10^{-5} M, Cl^- 10^{-2} M, NO_3^- 10^{-2} M, for MC4: 10^{-5} M Cl^-) by varying the pH of the 1mM universal buffer solution. The slides were conditioned for \sim 2h in the respective solutions before taking the fluorescence spectra. Maximum protonation and deprotonation was achieved using 0.01 M HCl and 0.01 M NaOH, respectively.

4.3.8 Fluorescence Measurements.

The optical setup included an inverted fluorescence microscope (Olympus IX-71, Olympus, Center Valley, PA) with attached microspectrometer (Acton Microspec MS-2150) and PIXIS-512 cooled CCD camera (both from Princeton Instruments, Trenton, NJ). The microspectrometer allows simple switching between direct imaging (non-dispersed) and spectral imaging (dispersed) modes. A mirror and a diffraction grating are attached to the motorized computer-controlled turret providing fast switching capability, thus the same camera can be used for both direct and spectral imaging.

A fast wavelength switch DG-4 (Sutter Instrument, Novato, CA) with 300 W xenon arc lamp and 535 (\pm 25) nm filter was used a light source. A filter cube consisted of 565 nm dichroic mirror and 600 nm long-pass emission filter. The microscope was equipped with 40x/0.17 objective (UPlanSApo, Olympus, Center Valley, PA).

The camera and the spectrometer were controlled by a PC running WinSpec32 software (Princeton Instruments, Trenton, NJ) in slave mode. A custom-programmed microcontroller was used to control DG-4 and generate triggering signals for the CCD camera. The detection was performed with 200 ms pulse of excitation light (550 nm) with simultaneous triggering of the camera shutter for 200 ms exposure.

The degree of protonation of films was calculated using the ratios of fluorescence intensity peaks at 710 nm (DiIC_{18}) and 675 nm (ETH 5418). The exposure time for spectral data acquisition was 40 msec.

4.3.9 Stability Constant Measurements

The sandwich membrane was made by pressing two membrane disks (one without ionophore (TDMACl 7 mmol/kg) and one carrying ionophore (15 mmol/kg MC3 or 10 mmol/kg MC4 and 7mmol/kg TDMACl)) within 2 mV individual potential together, after blotting them individually with dry tissue. This membrane was then pressurized using a spatula. Obtained sandwich membrane was visibly checked to make sure no air bubbles are trapped between the disks. This membrane was mounted on the Philips electrode body, with the disk without ionophore facing the sample. The inner filling solution contained 0.01 M KCl. Potential is read immediately after mounting onto the electrode, immersed in a solution similar to the inner filling solution.

The stability constant (β) was calculated using the following equation¹¹,

$$\beta = \left(L_T - \frac{nR_T}{z_i} \right)^{-n} \exp\left(\frac{E_m z_i F}{RT} \right) \quad (2)$$

where $E_m = E_{with\ ionophore} - E_{without\ ionophore}$, L_T is the total ionophore concentration, R_T is the total ion-exchanger concentration, n is the stoichiometry of the ion- ionophore complex, z_i is the charge of the ion, and all other symbols have their usual meaning.

All experiments were conducted at ambient temperature (23 ± 2 °C).

4.4 Results & Discussion

The response of the membranes based on MC3 ionophore was studied initially to evaluate the use of pulstrodes as a general procedure to characterize the selectivity of carrier based anion selective electrodes. As stated in the experimental section the pulstrode potentials were monitored in 2 different modes namely, applied current mode and zero current mode. We established in one of the earlier papers that the

potentials of the zero current mode are least affected by possible artifacts of the current pulse applied across the solution/membrane interface.¹⁵ Therefore this became the preferred mode to obtain selectivity coefficients. However, when calibration graphs are plotted, non-Nernstian slopes were observed in zero current mode for less discriminated ions such as Cl^- , NO_3^- , and OH^- (data not shown), while in the applied current mode these ions exhibit calibration plots with the slopes close to Nernstian (Figure 4.2). One could anticipate this observation, since, during the zero current mode previously extracted background ions exchange with the ion of interest via zero current counter diffusion ion-exchange process. This could lead to a super-Nernstian response slope that is not visible in the applied current mode. Further, in the zero current mode, at high I^- activities slope with an opposite sign is observed due to Donnan failure²¹. Therefore in this mode the selectivity coefficients were calculated at lower activities where Nernst response is observed.

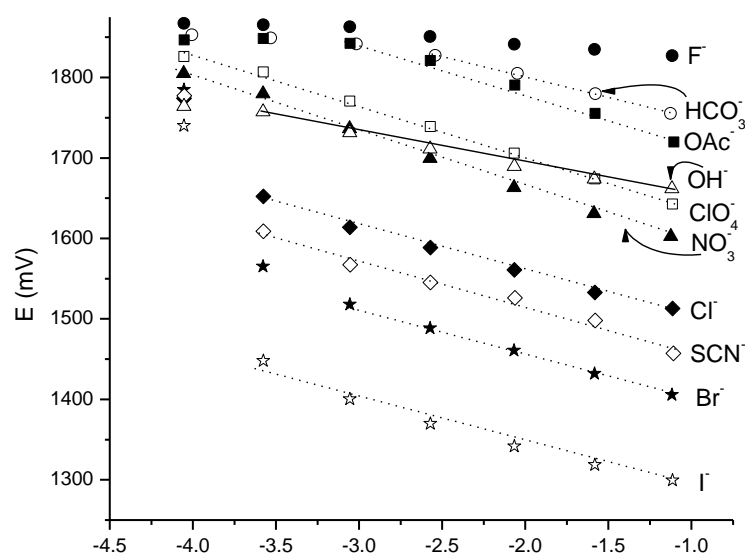


Figure 4.2: Response of pulstrode containing MC3 carrier, towards K^+ salts of I^- (slope = -59.04 mV/dec), SCN^- (slope = -57.09 mV/dec) and Na^+ salts of Br^- (slope = -57.79 mV/dec), Cl^- (slope = -56.19 mV/dec), NO_3^- (slope = -69.34 mV/dec), OH^- (slope = -39.12 mV/dec), ClO_4^- (slope = -63.89 mV/dec), OAc^- (slope = -63.62 mV/dec), HCO_3^- (slope = -51.3 mV/dec), F^- (slope = -16.14 mV/dec). Potential measured in applied current mode ($20 \mu\text{A}$) with Na_2SO_4 (0.01 M) as background electrolyte.

Figure 4.3 compares the selectivity coefficients for MC3 obtained via both pulstrode detection modes to the ones obtained using optical sensors, and published values via traditional ISE. Results acquired using the pulstrodes are in good agreement with selectivity coefficients within an order of magnitude except selectivity coefficients for Cl^- , SCN^- and OH^- . It has been known that selectivity coefficients are meaningful only if Nernstian electrode slope is observed for the ion of interest. Slight discrepancy in the selectivity coefficients of the aforesaid ions can be due to the non-Nernstian slope observed for the ions in the zero current mode.

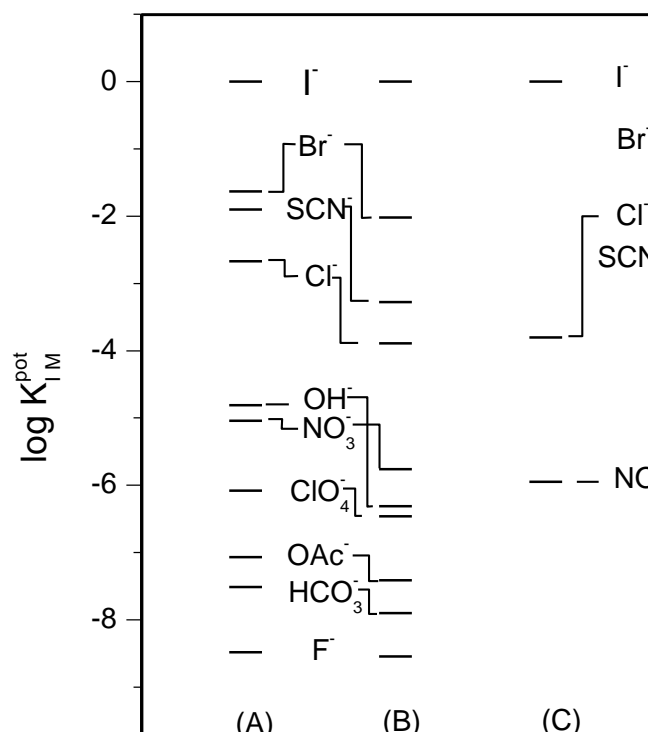


Figure 4.3: Experimental selectivity coefficients, ($\log K_{I,J}^{pot}$) for (A) I-selective PVC:o-NPOE (1:2) pulstrode membranes containing MC3 and ETH500 potentials measured under zero current conditions. (B) Same membrane as in A, potentials measured under applied current conditions. (C) I-selective PVC:DOS (1:2) optodes MC3, chromoionophore VII and the reference dye. (D) Cl-selective PVC:o-NPOE (1:2) potentiometric membranes containing MC3 and TDMACl¹

It has been demonstrated that the selectivity based on the same carrier, determined using electrodes and optodes can be compared, if the optode selectivities are obtained graphically as the horizontal distance at 0.5 fraction of unprotonated chromoionophore (α) of the normalized response curve on a logarithmic activity scale.¹⁹ The optical sensing films based on MC3 has been first developed by Bachas et al²⁰ and has been studied in detail by Bakker and his co-workers^{4,7-9}. They demonstrated that the optodes fabricated by former suffered from high levels of Na interference under physiological conditions and subsequently fabricated MC3 optodes with dramatically reduced Na interference⁴. The same experimental procedure followed by Bakker, was employed in developing and testing the MC3 optodes in this paper.

Optode response depended on the coextraction equilibrium of H^+ and X^- (I^- , Cl^- , NO_3^-) from aqueous sample into the organic sensing phase, following the response function⁴

$$a_{X^-} a_{H^+} = K_{coex}^{-1} \left(\frac{1-\alpha}{\alpha} \right) \frac{(1-\alpha)Ind_T}{\{L_T - n(1-\alpha)Ind_T\}^n} \quad (3)$$

where a_X and a_H are the sample activities of the measured anion and hydrogen ion, respectively. K_{coex} is the coextraction constant for the equilibrium, α is the mole fraction of unprotonated chromoionophore (experimentally determined), Ind_T and L_T are the total concentrations of chromoionophore and ionophore, respectively. n is the assumed complex stoichiometry for MC3 ionophore complex. The theoretical response according to eq.(1) fit the data well for $n=1$. The selectivity coefficients were obtained as the horizontal distance at $\alpha = 0.5$. As shown in Figure 4.2, the measured selectivities obtained using MC3 optical sensors are in excellent agreement with the pulstrode results. Further, unbiased selectivity values obtained with pulstrodes agree well with the published values, thus confirming the validity of the use of pulstrodes in measuring the unbiased selectivity of anion carriers.

As pointed out in the introduction, one of the main objectives of this paper is to characterize MC4 as a neutral carrier for anions. We employed the traditional ISEs and pulstrodes conditioned in 10 mM NaCl in order to obtain the anion selectivity

sequence and the respective selectivity coefficients using separate solution method. Unlike in the case of MC3 pulstrodes, only zero current detection mode provided linear responses towards I^- with pulstrode membranes containing MC4, rendering it the only detection mode that provided reliable results.

In Figure 4.4A, the typical responses of MC4 ionophore towards various anions are shown. The corresponding electrode slopes (in both traditional ISE and pulstrode) for most of the measured ions are close to Nernstian, indicating that the membrane reversibly responds to them. The potential difference between I^- and SCN^- translates into a selectivity coefficient $\log K_{\text{I},\text{SCN}}^{\text{pot}} = -3.62$ (Figure 4.4), which may indicate that this carrier could be the most selective I^- carrier available to date.

Moreover OH^- and Cl^- are highly discriminated with respect to I^- , therefore its interference towards a measurement will be minimal. Unfortunately due to the strong complexation of I^- by MC4, Na^+ interference is still visible at high I^- concentrations in both pulstrodes as well as traditional ISEs. As seen in the calibration plot, all highly discriminated ions (OH^- , OAc^- , HCO_3^- , F^-) produced sub-Nernstian slopes when tested using pulstrodes. These subsided around the same potential value, providing similar selectivity co-efficients.

Further, when tested for OH^- , OAc^- , HCO_3^- , F^- using the traditional ISE, the slope was strongly sub-Nernstian. This means that potential on the electrode was influenced by the thermodynamic equilibrium between the membrane and adjacent solution interface.²¹ Thermodynamic equilibrium is fulfilled when phase transfer kinetics and involved complex formation are fast with respect to the diffusion process involved. Since these ions are highly discriminated we likely worked under non-equilibrium conditions under which the observed potential values could be limited by the kinetics of the reaction.

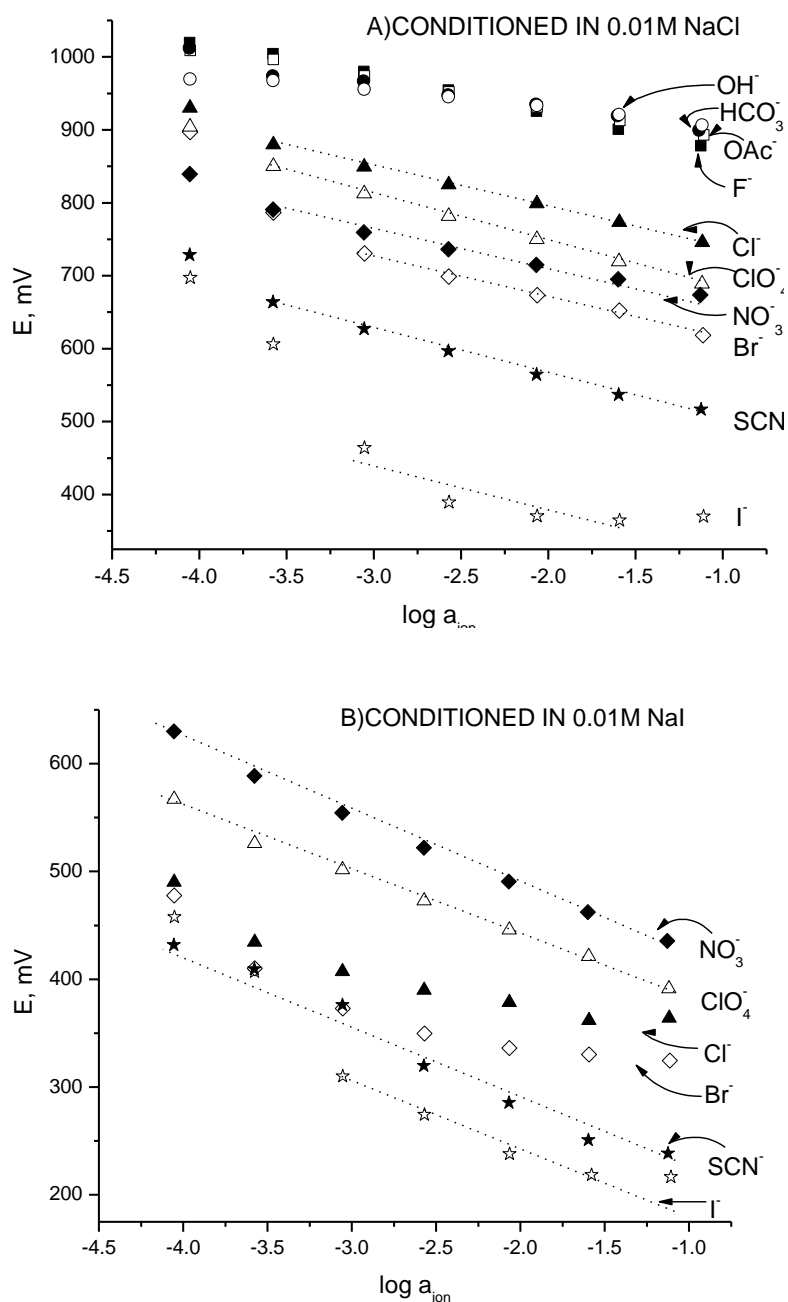


Figure 4.4: Response of pulstrode containing MC4 carrier, (A) conditioned in 0.01 M NaCl and (B) conditioned in 0.01 M NaI, towards Na^+ salts of I^- (slope = -64.9, -63.0 mV/dec), SCN^- (slope = -60.6, -57.9 mV/dec), Br^- (slope = -55.9, -48.8 mV/dec), Cl^- (slope = -53.8, -35.1 mV/dec), NO_3^- (slope = -53.5, -62.6 mV/dec), ClO_4^- (slope = -63.8, -57.7 mV/dec), OH^- (slope = -24.5 mV/dec), OAc^- (slope = -41.8 mV/dec), HCO_3^- (slope = -34.8 mV/dec), F^- (slope = -52.3 mV/dec). Slopes are given in order (A), (B) respectively. Potential measured in zero current mode (15 μA) with Na_2SO_4 (0.01 M) as background electrolyte.

Optodes based on coextraction principle, similar to the ones developed using MC3, were fabricated using MC4 ionophore as well. Unfortunately, due to protonation of the reference dye upon conditioning of the optical film by the buffer, very little absorbance change was observed upon the change in pH of the testing solution. Furthermore complete deprotonation was not observed even in 10 mM NaOH solution. Thus the optical films based on coextraction were found to be inappropriate for the development of optodes using MC4.

The outcome of optodes suggests that the complex stability of the MC4 ionophore is even higher than the complex stability of MC3. This behavior was more carefully analyzed by assessing the complex formation constants using the sandwich membrane method.¹¹⁻¹³ Sandwich membrane experiments were performed for both ionophores, MC3 and MC4.

MC3 membrane contained 47 mol% anion-exchanger. It has been shown earlier that 1:2 complex of $[(MC3)_2Cl^-]$ is preferred over the 1:1 complex when excess ionophore is present.⁴ The formation constant of L_2Cl^- was determined to be $\log \beta_2 = 11.30 \pm 0.06$. Bakker *et al* studied the same ionophore under similar conditions reported the formation constant $\log \beta_2 = 13.4$.⁴ The discrepancy could be due to the difference in the plasticizer used. The o-NPOE was used in our experiments since we are more interested in keeping the membrane features similar to the pulstrode membranes. As mentioned before there are some experimental difficulties using DOS in the pulstrode membranes, owing to its incompatibility with high concentration of ETH500¹⁵. Polar plasticizer, o-NPOE has a higher dielectric constant which can alter the divalent/monovalent selectivity ratio, favoring divalent species because of the increased polarity of the membrane. Lower formation constant value obtained in o-NPOE membrane could be a result of this preference.

Properly determined selectivity coefficients for neutral carrier based membranes are typically related to the stability constants of the ion-ionophore complex in the membrane and the membrane concentration of ionophore and ion exchangers. As a consequence the selectivity coefficient can be illustrated using the equation below.²¹

$$K_{IJ}^{pot} = K_{IJ} \frac{(\beta_{JL_n})^{z_I/z_J}}{\beta_{IL_n}} \cdot \frac{R_T}{Z_I [L_T - n_I (R_T/z_I)]^{n_I}} \left(\frac{z_J [L_T - n_J (R_T/z_J)]^{n_J}}{R_T} \right)^{z_I/z_J} \quad (4)$$

where K_{IJ} is the equilibrium constant for the ion-exchange reaction between uncomplexed primary and discriminated ions between the sample and organic phase. L_T and R_T are the total concentrations of ionophore and ion-exchanger, β_{IL} and β_{JL} are the overall complex formation constants of primary and discriminated ions with ionophore L in the membrane phase. In case of equal charge of the primary and discriminated ion and equal stoichiometry of their complex formation constants, equation 2 can be simplified to:

$$K_{IJ}^{pot} = K_{IJ} \frac{\beta_{JL_n}}{\beta_{IL_n}} \quad (5)$$

Thus the observed selectivity becomes directly proportional to the ratio of the formation constants of the involved complexes. With the use of this relationship overall complex formation constant of $(MC3)_2I^-$ is determined as $\log \beta_2 = 11.55$.

Two sandwich membrane experiments were performed with MC4 ionophore, one with 40 mol% and the other with 140 mol% anion exchanger. The potentials observed clearly pointed out that first experiment demonstrated much stronger stabilization compared to the second. Therefore it is assumed that, MC4 resembling its counterpart MC3, which complexes with Cl^- , with stoichiometry 1:1 and 2:1. From the sandwich experiment data the overall complex formation constant for $[(MC4)_2Cl]^-$ was determined as $\log \beta_2 = 16.58 \pm 0.282$, while the equilibrium constant⁴ for the formation of $[MC4Cl]^-$ was $\log K_1 = 5.33 \pm 0.046$. The formation constant determined here is several orders of magnitude higher than the $\log \beta_2$ value found for MC3 complex. Comparatively high binding constant is consistent with the failure to produce functional optodes based on coextraction principle. When considering I^- complex of MC4, Hawthorne *et al* reported on the availability of $[MC4I_2]^{2-}$ complex using x-ray

diffraction studies¹⁰. Therefore using equation 2 the formation constant of $[\text{MC4I}_2]^{2-}$ was determined as 17.46 ± 0.282 .

In a previous communication we established that the conditioning solution has no effect on the selectivity coefficients determined using pulstrodes.¹⁴ This was credited to having no ion exchangers in the pulstrode membrane, which prevented the spontaneous extraction/release of ions to/from the membrane. Accordingly, same selectivity coefficients were expected from the pulstrode membrane that were conditioned using the primary ion, I⁻. Even though Nernstian slope was observed for most of the ions (Figure 4.4B) the selectivity coefficients were reduced remarkably. As shown on the comparison diagram in Figure 4.5, selectivity coefficients found using NaI conditioned pulstrode membranes are smaller than the ones determined with the pulstrode membrane conditioned in NaCl. However, the selectivity coefficients attained using latter is in good agreement with the ones obtained using traditional ISE. As observed before we detected the improvement of the selectivity with the pulstrode over the traditional ISEs.

It is possible the cause of poor performance of the NaI conditioned MC4 membrane was due to Donnan failure. Owing to the strong complexation of I⁻ by the ionophore, this could be coextracted to the membrane with its counter ion even to a membrane with no ion exchange properties. Therefore, a limitation in the use of pulstrodes for obtaining unbiased selectivity is encountered here. Apparently if the complex formation constant is very high the unbiased selectivity is not observed due to the presence of primary ions in the membrane.

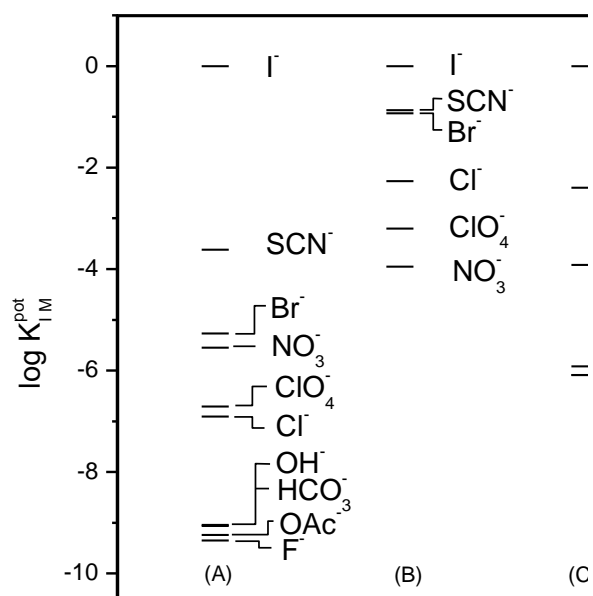


Figure 4.5: Experimental selectivity coefficients, ($\log K_{I,J}^{pot}$) for (A) I-selective PVC:o-NPOE (1:2) pulstrode membranes containing MC3 and ETH500 potentials measured under zero current conditions. (B) Same membrane as in A, potentials measured under applied current conditions. (C) I-selective PVC:DOS (1:2) optodes MC3, chromoionophore VII and the reference dye. (D) Cl-selective PVC:o-NPOE (1:2) potentiometric membranes containing MC3 and TDMACl¹

4.5 Conclusion

In this paper, the use of a pulstrode is established as a method to determine unbiased selectivity of neutral anion carriers. The unbiased selectivity of a new carrier MC4 was determined using this method and traditional potentiometric measurement. As expected MC4 selectivity towards I⁻ was found to be excellent and higher than that for MC3.

A drawback of the pulstrode method in determining unbiased selectivity has been encountered. High complex stability of [(MC4)I₂]⁻ complex, which resulted in coextraction of I⁻ into the membrane with its counter ion, affected the selectivity. Nonetheless, this high complex stability constant for ion-ionophore complexes are rarely observed, therefore this drawback will be of less importance.

4.6 Reference

- (1) Badr, I. H. A.; Diaz, M.; Hawthorne, M. F.; Bachas, L. G. *Anal. Chem.* **1999**, *71*, 1371-1377.
- (2) Badr, I. H. A.; Johnson, R. D.; Diaz, M.; Hawthorne, M. F.; Bachas, L. G. *Anal. Chem.* **2000**, *72*, 4249-4254.
- (3) Johnson, R. D.; Badr, I. H. A.; Diaz, M.; Wedge, T. J.; Hawthorne, M. F.; Bachas, L. G. *Electroanalysis* **2003**, *15*, 1244-1250.
- (4) Ceresa, A.; Qin, Y.; Peper, S.; Bakker, E. *Anal. Chem.* **2003**, *75*, 133-140.
- (5) Malon, A.; Radu, A.; Qin, W.; Qin, Y.; Ceresa, A.; Maj-Zurawska, M.; Bakker, E.; Pretsch, E. *Anal. Chem.* **2003**, *75*, 3865-3871.
- (6) Radu, A.; Telting-Diaz, M.; Bakker, E. *Anal. Chem.* **2003**, *75*, 6922-6931.
- (7) Wygladacz, K.; Bakker, E. *Anal. Chim. Acta* **2005**, *532*, 61-69.
- (8) Xu, C.; Qin, Y.; Bakker, E. *Talanta* **2004**, *63*, 180-184.
- (9) Wygladacz, K., Bakker, Eric *Analyst* **2007**, *132*, 268-272.
- (10) Hawthorne, M. F. Y., X; Zheng, Z. *Pure & Appl. Chem.* **1994**, *66*, 245-254.
- (11) Mi, Y. Bakker, E. *Anal Chem* **1999**, *71*, 5279-5287.
- (12) Qin, Y. Mi, Y. Bakker, E. *Anal. Chim. Acta* **2000**, *421*, 207-220.
- (13) Shultz, M. M. S., O.K.; Mokrov, S.B.; Mikhelson, K.N *Anal. Chem.* **2002**, *74*, 510-517.
- (14) Perera, H.; Shvarev, A. *J. Am. Chem. Soc.* **2007**, *129*, 15754-15755.
- (15) Perera, H.; Shvarev, A. *Anal. Chem.* **2008**, *80*, 7870-7875.
- (16) Shvarev, A.; Bakker, E. *Anal. Chem.* **2003**, *75*, 4541-4550.
- (17) Makarychev-Mikhailov, S., Shvarev, A., Bakker, E. *J. Am. Chem. Soc.* **2004**, *126*, 10548 - 10549.
- (18) Meier, P. C. *Anal. Chim. Acta* **1982**, *136*, 363.
- (19) Bakker, E. *Anal. Chim. Acta* **1997**, *350*, 329-340.
- (20) Badr, I. H. A.; Johnson, D.; Diaz, M.; Hawthorne, M. F.; Bachas, L. G. *Anal. Chem.* **2001**, *73*, 134.
- (21) Bakker, E.; Buhlmann, P.; Pretsch, E. *Chem. Rev.* **1997**, *97*, 3083 - 3132.

CHAPTER 5

**PULSED GALVANOSTATIC CONTROL OF SOLID-STATE POLYMERIC
ION-SELECTIVE ELECTRODES**

Hasini Perera, Katherine Fordyce, Alexey Shvarev*

Analytical Chemistry

1155, 16th Street N.W, Washington, DC 20036

Volume 79 (2007), Issue 12, 4564-4573

5.1 Abstract

We report on galvanostatically controlled solid-state reversible ion-selective sensors for cationic analytes utilizing conducting polymer as a transduction layer between the polymeric membrane and electron-conductive substrate. The instrumental control of polymeric membrane ion-selective electrodes based on electrochemically induced periodic ion extraction in alternating galvanostatic/potentiostatic mode was introduced recently creating exciting possibilities to detect clinically relevant polyions such as heparin and protamine and drastically improve of the sensitivity of ion-selective sensors limited by the Nernst equation. The present study forms the basis for development of reliable, robust, and possibly maintenance-free sensors that can be fabricated using screen-printing technology. Various aspects of the development of solid-contact galvanostatically controlled ISEs with a conducting polymer as a transduction layer are considered in the present work on example of a model system based on sodium-selective membrane. The protamine-selective solid-contact sensor was fabricated and characterized, which represents the next step towards commercially viable polyion sensing technology. A substantial improvement of a low detection limit (0.03 mg L^{-1}) was achieved. A simplified diffusion-based theoretical model is discussed predicting the polarization at the interface of conducting polymer and the membrane, which can cause the disruption of the sensor response function at relatively small current densities.

5.2 Introduction

There is a growing interest in the application of ion-selective electrodes (ISEs) under nonequilibrium conditions.¹ In the past decade several new transduction schemes for polymeric ISEs have been introduced,²⁻⁸ which could not be carried out within passive equilibrium readout techniques. The term “dynamic potentiometry” has been proposed to describe the response mechanism of ISEs working under non-equilibrium conditions.⁹

Electrochemically controlled ion transfer at the membrane/sample interface and in the bulk of the membrane has resulted in the development of several new sensor modalities.¹⁰ Recently, a new nonequilibrium detection technique was introduced based on periodic electrochemically controlled ion extraction into a polymeric membrane¹¹. Spontaneous ion-exchange was eliminated through the use of a membrane doped with an inert lipophilic electrolyte that did not possess ion-exchange properties. The ion uptake and subsequent stripping were induced by alternating current and potential pulses.⁵ One of the most important advantages of this method was the comprehensive instrumental control over the concentration polarization in the aqueous phase at the sample/membrane interface. The term pulstrodes was proposed for this type of ion-selective sensors.^{12, 13}

This new electrochemical technique yields a remarkable improvement in sensitivity,¹³ and allows one to perform multianalyte detection with a single sensor,⁵ distinguish activity and total concentration of an analyte,¹⁴ determine a concentration of polyionic compounds,⁶ and detect surface binding events. The most promising biomedical applications of these ion-selective sensors include continuous reversible detection of anticoagulants¹⁵ and accurate determination of small variations in blood electrolyte composition¹³ using point-of-care devices.

However, these remarkable achievements were developed with so-called liquid-contact ISEs, which have an internal reference electrode and internal reference solution (inner filling solution) in contact with the ion-selective membrane. On the one hand, applications of ISEs in biomedical and clinical analysis require reliable, robust, and ideally maintenance-free sensors. On the other hand, mass production of miniature and inexpensive sensors implies technological processes such as screen- and ink-jet printing, which are hard to apply to common liquid-contact ISEs.

Solid-contact ISEs with a conducting polymer (CP) ion-electron transduction layer represent a promising alternative to liquid-contact ISEs in terms of both function and manufacturing. These ISEs have been a subject of intensive research over the past decade.¹⁶ Conducting polymers demonstrate a well-defined pathway of ion-to-electron

transduction in combination with substantial redox capacitance, which has proven to be one of the major factors affecting potential stability of a solid-contact electrode. Several conducting polymers have been examined as intermediate transduction layers including poly (aniline), poly (pyrrole), poly (3,4-ethylenedioxythiophene), and poly (3-octylthiophene).¹⁶

The performance of solid-contact polymeric membrane ISEs under continuous galvanostatic polarization was studied recently.¹⁷⁻¹⁹ An improvement in low detection limits of chloride, calcium, and potassium-selective ISEs was observed and was attributed to the compensation of ion fluxes in the membrane/sample system by externally applied constant currents. However, the polarization current was in the range of nanoamperes with the corresponding current density¹⁷⁻¹⁹ below $0.1 \mu\text{A cm}^{-2}$. The charge passing under these conditions did not significantly affect the membrane/CP interface.

In contrast, the method based on galvanostatically induced ion extraction into ISE membranes^{5, 6} which do not possess ion-exchange properties, requires much higher currents with corresponding current densities^{5, 6, 13-15} higher than 0.1 mA cm^{-2} . Higher current density is essential for maintaining a sufficiently high concentration of the extracted ions at the interface in the membrane phase comparable to that in the potentiometric ISE membrane (about 10 mmol kg^{-1}). Indeed the response mechanism of pulsed galvanostatic ISEs implies a substantial polarization and ion uptake at the sample/membrane interface. Therefore, significant polarization caused by ionic fluxes at CP/membrane interface can be expected.

The study is focused on various aspects of the development of solid-contact galvanostatically controlled ISEs with conducting polymers such as poly(3,4-ethylenedioxythiophene)-poly(styrene sulfonate) (PEDOT:PSS) and poly (pyrrole) (PPy) as transduction layers. In the present work a sodium-selective solvent polymeric membrane was chosen as a simple model system because a liquid-contact galvanostatically controlled ISEs based on sodium ionophore 4-tert-butylcalix[4]arene-tetraacetic acid tetraethyl ester were extensively characterized

earlier.⁵ The membrane composition and experimental methodology used here was the same as in the earlier study.⁵

One of the most promising applications of the pulsed galvanostatic control of the ISEs with plasticized polymeric membranes is a continuous monitoring of polyionic compounds such as anticoagulant heparin and its antidote protamine in whole blood specimens during the surgery.^{6, 15} Due to the high charge of the polyionic molecules a potentiometric polyion-selective electrode exhibited a negligible small slope of the response function, which makes the response practically independent on the polyion concentration.³ In contrast potentiometric membrane electrode doped with an ion-exchanger methyltridodecylammonium in a chloride form demonstrated a significant non-linear heparin response³ due to the continuous irreversible heparin extraction into the membrane phase. Similar membrane electrode was fabricated for the detection of polycation protamine using dinonylnaphthalene sulfonate in sodium form.²⁰ However, because of irreversible nature of the extraction process the electrode potentials continuously drifted and after prolonged exposure to the solutions containing polyions the electrodes lost their response function demonstrating negligible slope close to the calculated according Nernst equation³.

The reversibility of the electrochemically induced ion extraction offers tremendous advantage over potentiometric polyion-selective electrodes.⁶ The continuous reversible detection of protamine in the whole blood specimens was demonstrated earlier with liquid contact sensors¹⁵. Protamine ion-selective electrode used as an end-point detector created a possibility of determination of the heparin concentration via titration with protamine, utilizing very specific heparin-protamine interaction.¹⁵ In this work we attempted to fabricate a reversible protamine pulsed galvanostatic sensor with a conducting polymer transduction layer, which represents the next step towards commercially viable polyion sensing technology

Recently a voltammetric detection of heparin with CP-modified PVC membrane electrode was demonstrated²¹. In order to minimize the membrane resistance, which produced significant uncontrollable iR drop, a thin 3-5 μm membrane was used. The

reliability of this sensor in a real sample such as whole blood is highly questionable taking into account a high permeability of such a thin membrane layer for blood gases such as CO₂ and oxygen, which may affect the properties of a CP layer. In contrast, in constant current techniques the membrane resistance is much less significant and, therefore, much thicker membranes (hundreds of microns) can be used¹².

In addition, it was reported that the utility of CP-supported voltammetric membrane electrodes is limited to anionic analytes because the CP transduction layer can not couple a cation transfer²¹. We report here on a successful fabrication of CP-based solid contact sensors for cationic analytes such as sodium and polycation protamine.

5.3 Experimental Section

5.3.1 Reagents.

High molecular weight poly(vinyl chloride)(PVC), 2-nitrophenyl octyl ether (o-NPOE), sodium ionophore 4-tert-Butylcalix[4]arene-tetraacetic acid tetraethyl ester, tetradodecylammonium tetrakis-(4-chlorophenyl)borate (ETH 500), tetrahydrofuran (THF), pyrrole, poly(3,4-ethylenedioxythiophene)-poly(styrene sulfonate) (PEDOT:PSS), protamine sulfate (from herring) and all salts were purchased from Sigma – Aldrich (Milwaukee, WI). All other chemicals were purchased from VWR (West Chester, PA). Tetradodecylammonium dinonylnaphthalenesulfonate (TDDA-DNNS) was synthesized according the procedure described by Bakker and coworkers⁶. Aqueous solutions were prepared by dissolving the appropriate salts in deionized water (18.2 MΩ cm).

5.3.2 Membrane Preparation.

The membrane matrices contained polymer (PVC) and plasticizer (o-NPOE) in a ratio of 1:2 by weight. Sodium-selective membranes contained 10 mmol kg⁻¹ sodium ionophore and 72 mmol kg⁻¹ of the lipophilic salt ETH 500, with no additional ion-

exchanger added. Protamine-selective membranes contained 45 mmol kg⁻¹ of the salt TDDA-DNNS. The membrane films (~200 μm thick) were fabricated by solvent casting with THF as a solvent.

5.3.3 Liquid-contact electrodes.

The ion-selective membranes were cut with a cork borer (6.6 mm in diameter) from the parent membrane and incorporated into a Philips electrode body (IS-561, Glasbläserei Möller, Zurich, Switzerland) with the Ag/AgCl internal reference electrode. The inner filling solution contained 0.1M NaCl. The exposed membrane area was 0.08 cm².

5.3.4 Solid-contact electrodes.

The housings of the solid-contact electrodes (120 mm long and 12 mm in diameter) were fabricated from a PVC rod. The conductive substrate was a graphite rod (6 mm in diameter, 99.9% spectroscopic grade), which was installed into the electrode housing. The graphite surface was polished with 3 μm polishing alumina, washed with acetone, and then air dried.

In order to form a transduction layer with a conducting polymer, two different techniques were used. The PEDOT:PSS (Baytron-P) used here was a form of aqueous emulsion containing 1.8% wt. of PEDOT:PSS blend (PEDOT:PSS mass ratio of 1:2.5). A transduction layer of PEDOT:PSS was deposited on the graphite substrate by drop casting 25 μL of PEDOT:PSS solution and letting it air dry. After drying the conducting polymer films were conditioned in a 0.01 M NaCl solution for 24 hours. Assuming the average density of PEDOT:PSS²² of 1.5 g cm⁻¹, the calculated thickness of the polymeric film was 10 (±2) μm.

PPy was electro-polymerized from an aqueous solution of 0.05 M pyrrole and 0.1M NaCl. PPy films doped with chloride were prepared by continuous scanning of a potential from 0.0V to 1.0V using a scan rate of 20 mV/s for 45 min in a three electrode cell. After deposition, the electrodes were washed thoroughly with water.

PPy doped with $[\text{Fe}(\text{CN})_6]^{3-}$ (PPY- $[\text{Fe}(\text{CN})_6]^{3-}$) was obtained via a 40 s electropolymerization at 1 V in the solution of 0.5M pyrrole and 0.5 M $\text{K}_3[\text{Fe}(\text{CN})_6]$. After deposition, electrodes were soaked for 3 hours in water to remove the excess electrolyte. After deposition of a conducting polymer layer electrodes were conditioned in 1M NaCl for 24 hours, washed, and dried. The resulting PPy film thickness was 8-10 μm^{23} .

The DC resistance of the dry PEDOT:PSS and PPy films were measured with a handheld multimeter as two coated electrodes were pressed against each other. The resistance did not exceed 50 Ohm/cm².

The ion-selective membranes were cut with a cork borer (6.6 mm in diameter) from the parent membrane, soaked in THF for a few seconds, pasted on top of the deposited conducting polymer layer, and left to air dry for 24 hours. The effective membrane area was 28 mm². Sodium and protamine-selective electrodes were conditioned overnight in 0.1M NaCl solution prior the experiment.

5.3.5 Chronopotentiometric measurements.

A conventional three-electrode cell was used for chronopotentiometric measurements. The membrane electrode was connected as a working electrode. A high surface area coiled platinum wire was used as a counter electrode. The reference electrode was a double junction Ag/AgCl electrode with saturated KCl as the inner solution and 1 M LiOAc as a bridge electrolyte.

The application of normal pulse chronopotentiometry to solvent polymeric membrane electrodes was introduced by Bakker and coworkers and is described in detail in a series of publications^{5, 14, 15}. A modified⁶AFCBP1 bipotentiostat (Pine Instruments, Grove City, MA) controlled by a PCI-6221 data acquisition board and LabView 7.1 software (National Instruments, Austin, TX) on a PC was used for measurements. A uptake current pulse of 1 s was followed by application of the stripping potential for 10 s. Sampled potentials were obtained as the average value during the last 10% of each 1 s uptake pulse.

According to the procedure described in the previous work,¹⁵ the value of stripping potentials were chosen to match the open-circuit potentials. The open-circuit potentials were recorded via a custom-built potentiometric station, which included several electrometric amplifiers (AD820, Analog Devices) connected to the 24-bit 8-channel data acquisition board NI-4351 controlled by the LabView software (National Instruments, Austin, TX)

5.3.6 Electrochemical Impedance Measurements.

Electrochemical impedance spectroscopy (EIS) was performed using a Solartron Electrochemical Interface (SI 1287) and an Impedance Analyzer (SI 1260) (Solartron, Hampshire, UK). Measurements were conducted on sodium-selective electrodes in the three electrode cell described above. The impedance spectra were recorded in a 10^{-2} M NaCl solution in the presence of 10^{-2} M MgCl_2 background within the frequency range 100 kHz – 10 mHz with a sinusoidal excitation signal of 100 mV amplitude. The results were fitted to an equivalent circuit using ZPlot software for Windows (Scribner Associates, Inc. Southern Pines, NC)

All experiments were conducted at ambient temperature (23 ± 2 °C). Activity coefficients were calculated according to Debye-Hückel formalism.²⁴

5.4 Theoretical Section

The theoretical basis for galvanostatically controlled ISEs is presented in two parts. In the first part, the simplified theoretical description of the behavior of a liquid-contact polymeric membrane sensor is considered. It is limited to single-charge ions and additional simplifications were made for the purposes of clarity. In contrast to previous work,^{5, 13} the contribution of the potential at the inner side of the membrane is considered because for solid contact electrode that interface is of importance. In the second part the analogous simplified model is derived for the solid-contact sensor with a conducting polymer as an ion-electron transducer.

5.4.1 Liquid contact interface.

A schematic representation of expected concentration profiles for a cation-selective pulstrode with an inner filling solution (IFS) is shown on Figure 5.1A. The polymeric membrane containing the lipophilic electrolyte R^+R^- separates two aqueous solutions. For simplicity we do not consider an ionophore mediated transport. We assume that a) the sample and inner filling solution contain the same 1-1 electrolyte I^+X^- and no discriminated ions are present in the sample, b) the concentration of the electrolyte is sufficiently high that no concentration polarization in the aqueous phases is observed, c) the diffusion coefficients of all ions in the membrane phase are equal, d) after prolonged application of stripping potential there are no other ions in the membrane but a background lipophilic electrolyte, d) activity coefficients in the membrane phase are unity. A cathodic current pulse of fixed width and amplitude is imposed across the membrane causing a flux of sample cations in the direction of the membrane. The current induces extraction of sample cations into the membrane, which is accompanied by the extraction of anions of the equal quantity of electric charge at the inner side of the membrane.

The phase boundary potentials at both sides of the membrane can be estimated on the basis of the equation:

$$E_i(pb) = \frac{RT}{zF} \ln \frac{k_i a_i(\text{phase 1}, pb)}{a_i(\text{phase 2}, pb)} \quad (1)$$

where k_i includes the free energy of transfer for an ion i , $a_i(\text{aq, phase 1})$ and $a_i(\text{org, phase 1})$ are the phase boundary activities of species i in the contacting phases (phase 1 on the left and phase 2 on the right), and R , T and F are the universal gas constant, the absolute temperature and the Faraday constant.

The potential across the membrane is the sum of phase boundary potentials at both sides of the membrane and Ohmic potential drop across the membrane:

$$E = E_{PB}^{(1)} + E_{PB}^{(2)} + iR_m \quad (2)$$

where i is the applied current and R_m is the membrane resistance. The symbols 1 and 2 refer to the phase boundary potentials at sample/membrane and membrane/IFS interfaces respectively.

The total flux at an interface is controlled by the applied current. For the simplified system considered here in which two membrane interfaces are connected in series, the total ion flux is equal to the cation flux at the sample/membrane interface and the opposite anion flux at the membrane/IFS boundary:

$$i / FA = J = J_I = -J_X \quad (3)$$

where F is the Faraday's constant, and A is the membrane area. In a one-dimensional case the rising concentration gradients in the membrane phase can be estimated using Fick's first law of diffusion. Thus, at the sample/membrane interface, the cation concentration gradient is given by:

$$J_I = -(D_m / \delta_m) \left[c_I^{org,bulk} - c_I^{org,pb} \right] \quad (4)$$

where D_m and δ_m are the diffusion coefficient and diffusion layer thickness in the membrane phase, $c_I^{org,pb}$ and $c_I^{org,bulk}$ are the concentrations of cations I^+ at the sample/membrane phase boundary and in the membrane bulk. The concentration gradient is calculated by subtracting the concentration at $x = \Delta x$ from concentration at $x=0$. Under applied current a thickness of the diffusion layer increases with time.

In an analogous manner the concentration gradient at the membrane/IFS boundary is:

$$J_X = -(D_m / \delta_m) \left[c_X^{org,pb} - c_X^{org,bulk} \right] \quad (5)$$

where $c_X(org, pb)$ and $c_X(org, bulk)$ are the concentrations of anions X^- at the membrane/IFS boundary and in the membrane bulk respectively. If the extracted ions are expelled from the membrane phase during the application of the constant stripping potential, the concentrations of sample electrolyte ions in the bulk of the membrane remain equal to zero and we can rewrite eq. 4 and eq. 5 as follows:

$$J_I = (D_m / \delta_m) c_I^0(org, pb) \quad (6)$$

$$J_X = -(D_m / \delta_m) c_X^0(org, pb) \quad (7)$$

The thickness of the diffusion layer can be estimated from:

$$\delta_m = 2\sqrt{D_m t} \quad (8)$$

where t is the duration of the applied current pulse (pulse width).

Inserting eq. 3 and 8 into eq. 6 and 7 and rearranging them with respect to the phase boundary concentrations of I^+ and X^- yields:

$$c_I(org, pb) = \frac{2\sqrt{t}}{iFA\sqrt{D_m}} \quad (9)$$

$$c_X(org, pb) = \frac{2\sqrt{t}}{iFA\sqrt{D_m}} \quad (10)$$

We assume that the phase boundary potential at the sample/membrane interface (Figure 5.1A) is dictated by the ratio of activities of I^+ cations in contacting phases and the phase boundary potential at the sample/IFS interface is determined by the ratio of activities of X^- anions. The potential across the membrane can be written using eq. 2 and inserting eq. 9 and 10 into eq. 1:

$$E = \frac{RT}{F} \langle \ln a_I(aq, pb) + \ln a_X(ifs, pb) \rangle + \frac{RT}{F} \ln \left[\frac{k_I k_X F^2 A^2 D_m}{4i^2 t} \right] + iR \quad (11)$$

According to this equation, the pulstrode potential depends on current amplitude i , current pulse duration t , and activities of I^+ and X^- in the sample and inner filling solution respectively. For an IFS of constant composition and a current pulse of fixed duration, eq.11 can be simplified to the Nernst equation. Ideally, if the concentration of the electrolyte IX is high and no concentration polarization in aqueous phases is observed, there are no limits for the liquid-contact pulstrode response in terms of duration and magnitude of the applied current pulse.

5.4.2 Solid contact interface with a conducting polymer as a transducer.

The result shown above may appear trivial, however, it is of importance for the solid-contact pulstrode in which the IFS is replaced with a conducting polymer layer (Figure 5.1B and C). As it will be seen, the CP phase has a high concentration of anions relative to the membrane and polarization in the CP phase is not expected as it is not expected for the IFS phase.

Despite their similarity, PPy and PEDOT:PSS are substantially different in terms of ionic composition. PPy contains polymeric molecules that are ion paired with relatively small anions such as chloride. The average length of PPy molecules lies with 26-48 monomer units.²⁵ The PEDOT:PSS complex contains PEDOT oligomers, which are 16-18 units long (MW 1000-2500 Da), and the high molecular weight polyelectrolyte PSS (MW 200,000 Da). Moreover, there is clear experimental evidence that PEDOT:PSS is indeed heterogeneous and contains a substantial excess of polyanionic PSS with protons as counterions.²² Thus, we may expect that the principal species responsible for charge transport across the membrane/CP interface are different for PPy and PEDOT:PSS.

The schematic representation of a solid contact pulstrode based on a PPy-like polymer, which upon reduction releases a small ion, is shown in Figure 5.1B. Under applied cathodic current the anions from the CP phase are extracted into the membrane. Upon application of stripping potential the reverse process takes place.

Due to the large molecular weight of the anionic component of PEDOT-PSS, we may expect that under applied cathodic current the lipophilic cations R^+ will be extracted from the membrane into the CP phase instead of extraction of anions released by the PPy into the membrane (Figure 5.1C).

We are going to consider these two situations separately. We assume that the oxidation-reduction reaction of a CP is fast and does not represent a rate limiting step within the time domain of the pulstrode response. This assumption appears to be reasonable because the electrochemical transistors²⁶ based on PEDOT-PSS demonstrated current modulation speeds approaching 200 Hz, which requires complete oxidation or reduction of a polymer film in every 5 ms cycle. In addition, when considering a PPy-like polymer, we assume that the CP is mostly present in the oxidized form CP^+ forming ion pairs with anions A^- . Based on these two assumptions we can consider a conducting polymer as a liquid polyelectrolyte with a certain bulk concentration of anions A^- . Eq. 2 can be transformed into:

$$E = E_{PB}^{(1)} + E_{PB}^{(2)} + iR_m + iR_{CP} + E_{PB}^{(3)} \quad (12)$$

The symbols 1 and 2 refer to the phase boundary potentials at sample/membrane and membrane/CP interfaces respectively. The additional terms are the resistance of a conducting polymer R_{CP} and the third phase boundary potential at the CP/metal interface. The ratio of activities of anions A^- in the membrane and the CP phase will dictate the phase boundary potential at the inner side of the membrane ($E_{PB}^{(2)}$). The resistance of the CP film is negligibly small compared to the resistance of a PVC membrane, which allows us to eliminate the R_{CP} in eq. 12.

We can consider a metal contact as an electrode on which a redox reaction takes place. The phase boundary potential at the CP/metal interface is determined by the Nernst equation and depends on the logarithm of the concentration ratio of oxidized /reduced forms of the CP. For a 10 μm thick PPy film we can determine the number of moles of reduced CP upon application of current of 10 μA for 1 s. The resulting charge value of 10^{-5} C is negligible when compared to the $7.2 \cdot 10^{-1}$ C required to reduce $7.5 \cdot 10^{-6}$

moles of PPy subunits units present in the film. This result suggests that the concentration ratio of oxidized and reduced forms of the CP remains constant as well as the phase boundary potential at CP/metal interface. If the abovementioned assumptions are valid, eq. 12 can be reduced to eq. 2 and eq. 11 is valid as well and can be rewritten as:

$$E = \frac{RT}{F} \langle \ln a_I(aq, pb) + \ln a_A(CP, pb) \rangle + \frac{RT}{F} \ln \left[\frac{k_I k_A F^2 A^2 D_m}{4i^2 t} \right] + iR \quad (13)$$

where $a_A(CP, pb)$ is the phase boundary activity of doping anions in the CP.

Experimental results obtained both by current-pulse and impedance methods suggest that the diffusion of ions in the conducting polymer is a rather slow process with apparent diffusion coefficients ranging from $2 \cdot 10^{-7}$ - $6 \cdot 10^{-7}$ for PEDOT:PSS²⁷ to $2 \cdot 10^{-9}$ - $4 \cdot 10^{-9}$ $\text{cm}^2 \text{s}^{-1}$ for poly (pyrrole).²⁸ These values are comparable to known diffusion coefficients of ions in PVC membranes of 10^{-8} $\text{cm}^2 \text{s}^{-1}$ and are much smaller than diffusion coefficients of ions in water (10^{-5} $\text{cm}^2 \text{s}^{-1}$). At the same time the concentration of doping anions in the conducting polymer phase is relatively high.

To predict a concentration gradient of anions A^- in the CP phase we can rewrite eq. 4 as follows:

$$J_A = -(D_{CP} / \delta_{CP}) \left[c_A(CP, bulk) - c_A(CP, pb) \right] \quad (14)$$

where CP refers to the corresponding parameters for the conducting polymer phase. We are interested in the situation in which the polarization in the CP phase is sufficient to reduce the $c_A(CP, pb)$ to zero. Inserting eq.3 and eq.8 into eq. 14 and rearranging gives us an expression for the combination of current amplitude and pulse width that will cause complete depletion of the phase boundary concentration of anions A^- for the known concentration of these ions in the CP phase:

$$i\sqrt{t} = \frac{FA\sqrt{D_{CP}}}{2} c_A(CP, bulk) \quad (15)$$

Assuming²⁹ the PPy density is 1.5 g cm^{-3} and taking into account that there is approx. 0.22 moles of A^- per each pyrrole subunit,³⁰ the calculated concentration of anions for poly(pyrrole) monomer units is 6 mol L^{-1} . A rough estimation of $i \cdot t^{1/2}$ for PPy with D_{CP} equal to $4 \cdot 10^{-9} \text{ cm}^2 \text{ s}^{-1}$ and membrane area of 0.28 cm^2 yields the value of $5 \cdot 10^{-3} \text{ A} \cdot \text{s}^{1/2}$ thus limiting the current to 5 mA for 1 s pulse with a corresponding current density of $18 \text{ mA} \cdot \text{cm}^{-2}$. This value far exceeds a required value of 0.1 mA cm^{-2} ,^{5, 6, 13-15} thus, no significant concentration polarization in the CP phase should occur.

In case of a PEDOT-like conducting polymer we may expect that the uptake of cations R^+ from the membrane takes place, causing the concentration gradient of the lipophilic electrolyte R^+R^- in the membrane phase (Figure 5.1C). The ratio of activities of the R^+ cations in the membrane and the CP phase will dictate the phase boundary potential. An equation similar to eq. 15 can be derived and in this case used to predict a concentration polarization in the membrane phase:

$$i\sqrt{t} = \frac{FA\sqrt{D_m}}{2} c_R(\text{org}, \text{bulk}) \quad (16)$$

Assuming a concentration of ETH 500 in the membrane phase of 72 mol L^{-1} , a diffusion coefficient of $D_m = 1 \cdot 10^{-8} \text{ cm}^2 \text{ s}^{-1}$, and a membrane area of 0.28 cm^2 we can estimate the value of $i \cdot t^{1/2}$ as approx. $8.8 \cdot 10^{-5} \text{ A} \cdot \text{s}^{1/2}$ with the corresponding current density $0.3 \text{ mA} \cdot \text{cm}^{-2}$. This value is comparable to the required $0.1 \text{ mA} \cdot \text{cm}^{-2}$ and indeed is substantially smaller than that for the for PPy-like transduction layer. This fact implies a serious limitation on the further developments of this type of sensor and it should be examined experimentally.

5.5 Results and Discussion

A large number of preliminary experiments demonstrated that the performance of sensors based on PPy doped with chloride ions is substantially lower than that for PPy-[Fe(CN₆)]³⁻. Thus, we report the data for the latter system only.

The curves shown in Figure 5.2 represent potential readings for a sequence of 20 cathodic current pulses of linearly increasing amplitude ranging from 0 to -20 μ A in aqueous solutions containing 0.01 M of the chlorides of Na⁺, K⁺, Ca²⁺, Mg²⁺, and LiOAc. The current-potential curve for the liquid contact electrode shown in Figure 5.2A was similar to the curve reported earlier.⁵ Despite the lower absolute potential values, the current-potential plots observed for solid-contact pulstrodes based on PPy-[Fe(CN₆)]³⁻ (Figure 5.2B) and PEDOT:PSS (Figure 5.2C) are quite similar to the response of their liquid-contact counterpart (Figure 5.2A). At currents higher than -19 μ A for liquid-contact and -15 μ A for solid-contact sensor, we observed a switch of selectivity demonstrated earlier¹⁵ between sodium and potassium due to the fact that at high currents ion transport is no longer assisted by the ionophore. Both solid contact sensors demonstrated good reproducibility of the potential readings with standard deviation lower than 0.5 mV.

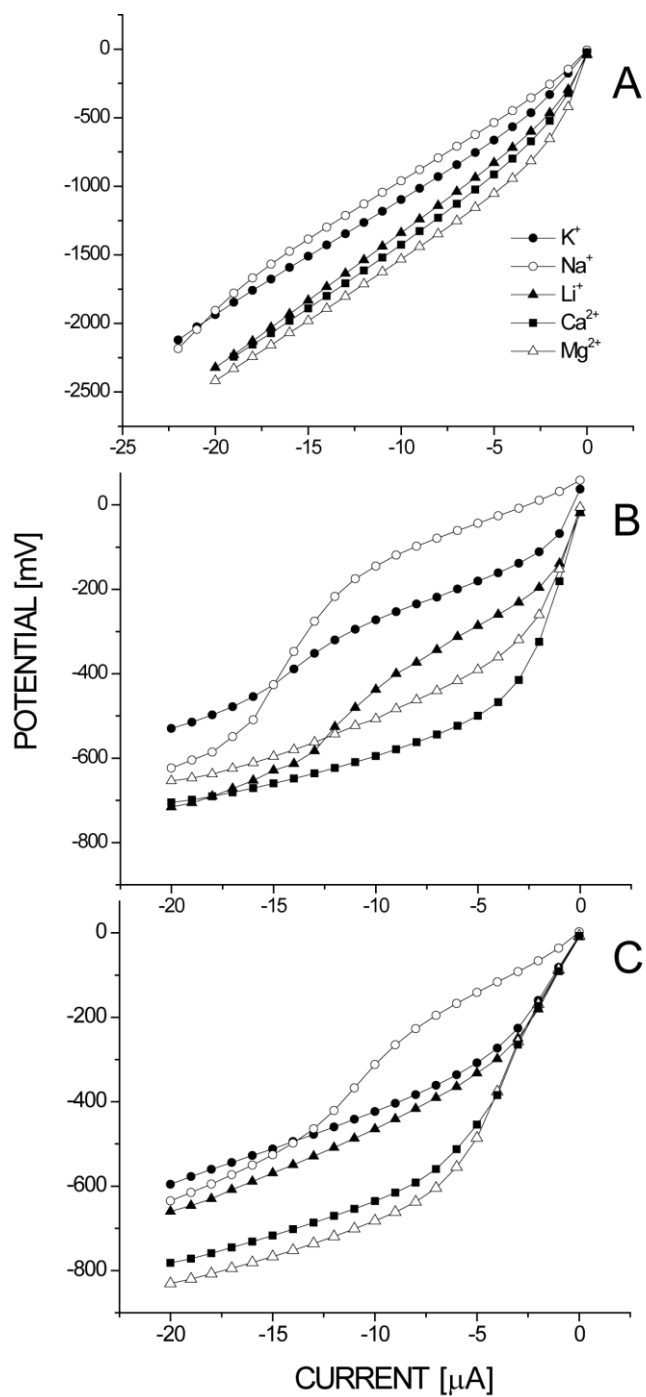


Figure 5.2. Pulsed chronopotentiograms for a sodium-selective membrane containing lipophilic electrolyte ETH 500 and sodium ionophore in separate solutions of 0.01 M KCl, NaCl, LiOAc, CaCl_2 and MgCl_2 . (A) The liquid-contact sensor (B) The solid-contact sensor with PPy- $\text{Fe}(\text{CN})_6$ as a transduction layer (C) The solid-contact sensor with PEDOT:PSS as a transduction layer.

In order to obtain a potential vs. concentration response the concentration of NaCl was varied from 10^{-7} M to 10^{-1} M in the presence of a 0.01 M MgCl_2 background at a constant current of $-7 \mu\text{A}$. The resulting calibration curves for solid-contact pulstrodes based on $\text{PPy}-[\text{Fe}(\text{CN})_6]^{3-}$ and PEDOT:PSS are shown on Figure 5.3A and Figure 5.3B respectively. Both sensors demonstrated a response similar to that reported for liquid-contact sodium-selective pulstrodes.⁵ Both graphs contain linear Nernstian-like region above 10^{-3} M NaCl with the slope of 59.6 mV/decade for PPy and 63.4 mV/decade for PEDOT:PSS transduction layer.

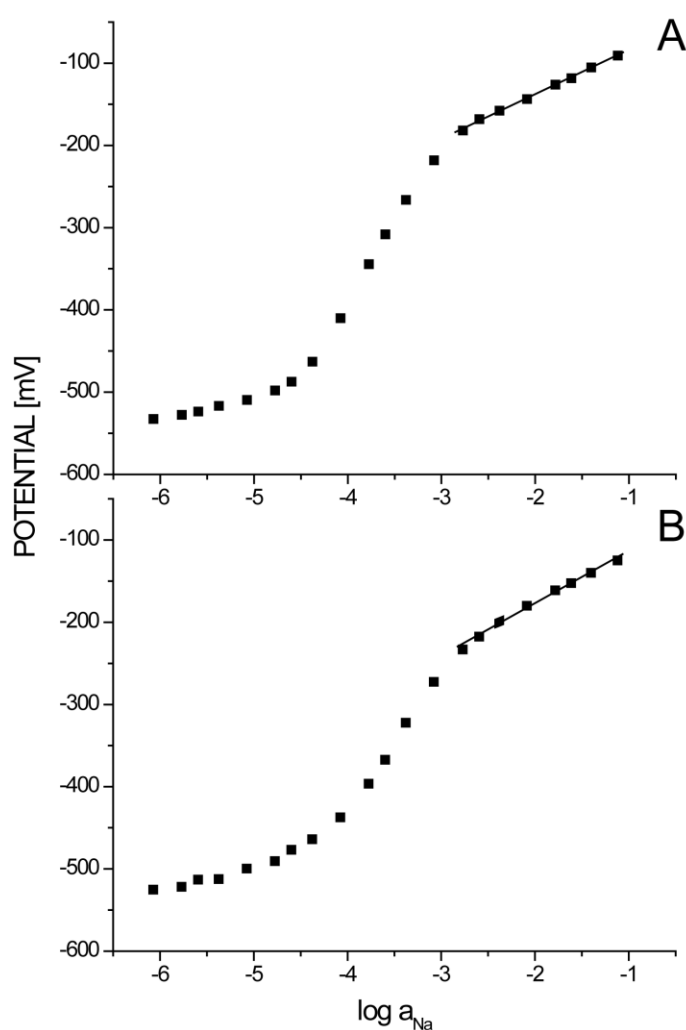


Figure 5.3. Response to sodium in presence of 0.01 M MgCl_2 at constant current of $-7 \mu\text{A}$, the pulse duration is 1 s. (A) The $\text{PPy}-\text{Fe}(\text{CN})_6$ solid-contact sensor. Solid line with slope of 59.6 mV/decade (B) The PEDOT:PSS solid-contact sensor. Solid line with slope of 63.4 mV/decade.

We used the separate solution method to determine apparent selectivity coefficients for the pulstrodes. Assuming the a Nernstian-like response at a constant current of $-7 \mu\text{A}$, the selectivity coefficients were calculated using the data shown in Figure 5.2 according the formula:³¹

$$\log K_{IJ}^{pot} = \frac{z_I F \{E_J - E_I\}}{2.303RT} + \log \left\{ \frac{a_I(aq)}{a_J^{z_I/z_J}(aq)} \right\} \quad (17)$$

where the primary ion is represented by I , the discriminated ion is represented by J , and z_I and z_J are the charges of respective ions. The E_I and E_J are observed potentials in solutions containing primary or discriminated ions alone with the activities $a_I(aq)$ and $a_J(aq)$ respectively.

The observed apparent selectivity coefficients are summarized in Table 5.1. For solid-contact pulstrodes based on PPy- $[\text{Fe}(\text{CN})_6]^{3-}$ and PEDOT:PSS, the apparent selectivity for Na^+ over K^+ , Ca^{2+} , and Mg^{2+} was comparable to that for the liquid-contact pulstrode. Both solid-contact sensors demonstrated surprisingly low selectivity for lithium compared to liquid-contact sensors. A possible explanation is that the CP layers may exhibit strong ion-exchange selectivity with respect to lithium. However, this assumption requires further investigation.

Table 5.1 Optimum logarithmic selectivity coefficients ($\log K_{Na,J}^{pot}$) obtained for sodium-selective galvanostatically controlled ion-selective sensors (pulstrodes).

Inner membrane interface	Discriminated ion			
	K^+	Li^+	Mg^{2+}	Ca^{2+}
Liquid-contact	-2.33	-7.82	-9.16	-7.66
PPY:FeCN	-2.43	-5.22	-6.96	-6.16
PEDOT:PSS	-2.86	-3.34	-6.94	-6.17

For sodium concentrations below 10^{-5} M, the low potentials we observed were due to complete depletion of sodium concentration at the sample side of the membrane and the resulting response to highly discriminated magnesium ions.^{5, 14} In the transition response area between 10^{-5} M and 10^{-3} M NaCl, applied currents induce a partial depletion of the sodium concentration at the sample side of the membrane with an apparent super-Nernstian slope.

We were particularly interested in the stability of the potentials in this region because of its practical importance for drastic sensitivity improvements^{12, 13} and polyion detection applications.^{6, 15} In contrast to pulsed galvanostatic sensors, the classic potentiometric ISEs exhibit strong drifts and poor reproducibility of the potentials observed in this region.³² This is because the associated diffusion gradients continuously change with time. Therefore, the measurements under such nonequilibrium conditions have limited analytical applicability. In contrast, the instrumental control of ion fluxes in the pulsed galvanostatic sensors yields stable and reproducible results.

The influence of stripping potential value on the stability of potential readings under applied current was previously evaluated.¹⁵ It was found that the lowest potential drift is observed when the stripping potential lies within a ± 20 mV window with respect to the open-circuit potential measured against the same reference electrode. In addition, it was found that the optimal value of the stripping potential corresponds to minimal value of the stripping current.¹⁵ In order to evaluate the influence of the stripping potential, we compared the potential drift of a PEDOT-based solid-state sensor in the super-Nernstian region at two distinctive stripping potentials. The pNa was 3.02 and 1 s current pulses of $-6 \mu\text{A}$ were applied. The results are shown in Figure 5.4. If the stripping potential of the sensor was held at 0.0 mV a significant potential drift of 2.8 mV min^{-1} was observed. When the stripping potential was set equal to the open-circuit potential of -224 mV, the drift of the potential readings was reduced to 0.5 mV min^{-1} , which was comparable to the experimental error. The stability of the recorded potential indicates complete stripping of the extracted ions back into the sample as well as the completion of the relaxation process at the membrane/CP interface.

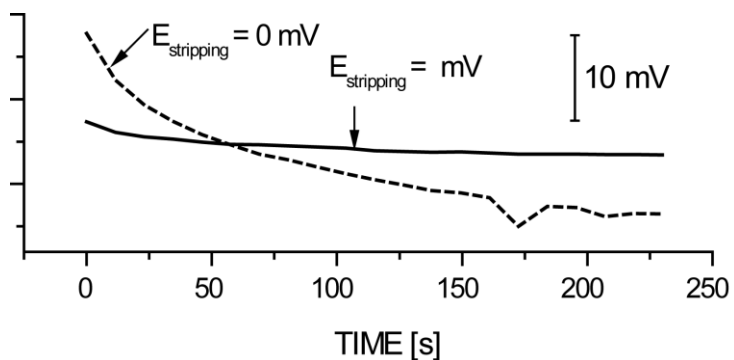


Figure 5.4. Potential stability of the PEDOT:PSS solid-contact sensor in 0.001 M NaCl solution in presence of 0.01 M MgCl_2 recorded at two different stripping potentials 0.0 mV and -224.0 mV. The latter is equal to open-circuit potential.

Both PPy-[$\text{Fe}(\text{CN})_6$] and PEDOT:PSS based sensors were studied at various concentrations of NaCl from 10^{-6} M to 10^{-1} M in the presence 0.01 M MgCl_2 background at constant current of $-6 \mu\text{A}$ (Figure 5.5). The PEDOT:PSS sensor demonstrated low short-term potential drift of 0.4 mV min^{-1} at $\text{pNa} = 3.02$. The long-term stability was satisfactory as well. The deviation between two consecutive measurements made within 24 hours did not exceed 1.5 mV. In contrast, we observed higher short-term potential drift of 1.2 mV min^{-1} for the PPy-[$\text{Fe}(\text{CN})_6$] based sensor at the same activity of sodium. Moreover, the PPy-[$\text{Fe}(\text{CN})_6$] based sensor exhibited poor long-term stability showing a continuous drift of the recorded potentials more than 20 mV over 24 hours.

It is possible the cause of poor performance of the PPy films was continuous degradation of the conducting polymer upon periodic reduction/oxidation cycles. As was shown using cyclic voltammetry³³, the redox capacity of the PPy film decreased to 50% after 50 reduction/oxidation cycles and completely diminished after 400 cycle. In contrast the PEDOT:PSS films exhibited very stable redox capacity that gradually decreased in the 1st 3 cycles and then remained constant through the 400th cycle. Moreover, results obtained by CV and EIS revealed that PEDOT is electrochemically more stable than PPy in presence of O_2 and CO_2 in the aqueous solution.³⁴

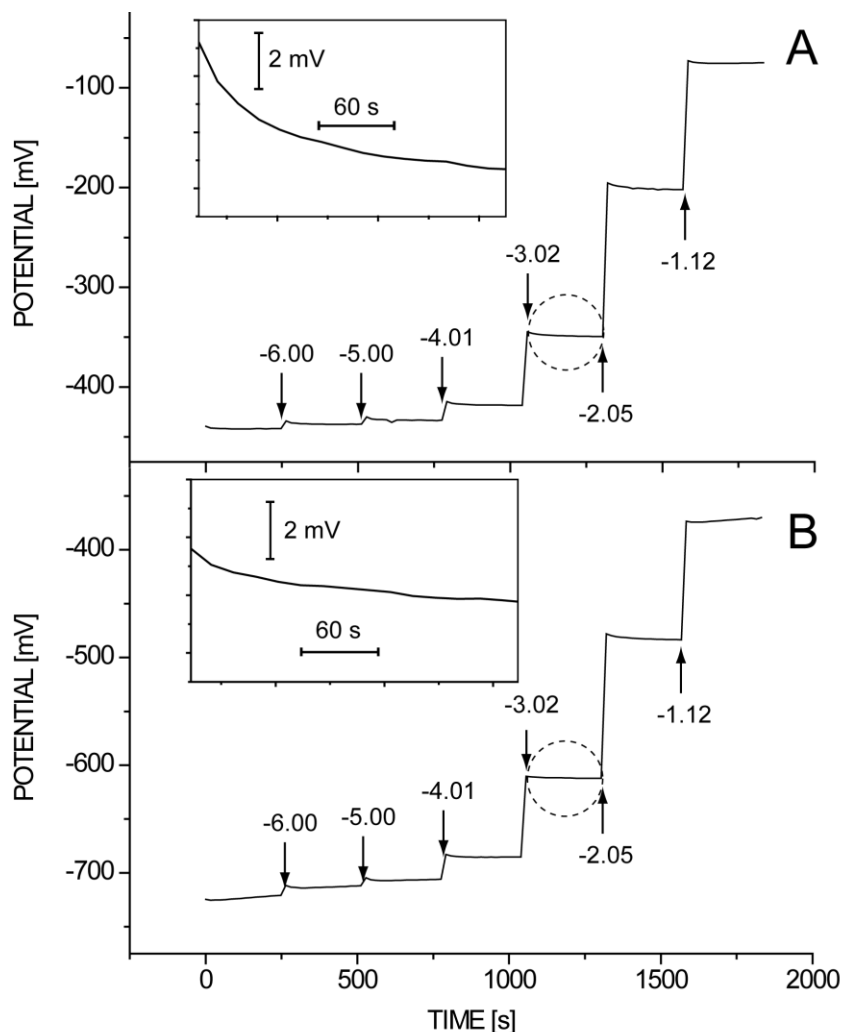


Figure 5.5. Time-dependent response of the sodium calibration (A) The PPy-Fe(CN)₆ solid-contact sensor. (B) The PEDOT:PSS solid-contact sensor. The numbers represent the corresponding log a_{Na} values. Magnified inset shows potential stability at log a_{Na} 3.02.

In order to investigate the possible contribution of charge transfer at the CP/membrane interface we studied impedance spectra of liquid and solid-contact sensors. The results of the impedance measurements in a 0.01M NaCl solution with a 0.01M MgCl₂ background electrolyte are presented in Figures 5.6A and 5.6B for liquid-contact and for solid-contact sensors respectively. The measurements were carried out with the potential values equal to the open-circuit potentials of the corresponding sensors. The equivalent circuit, which was used to fit the impedance spectra, is shown Figure 5.6A.

The circuit components are bulk resistance R_b and geometric capacitance C_g of the membrane, C_{dl} and R_{ct} represent capacitance of a double electric layer and charge transfer resistance, R_s is a solution resistance, and Warburg impedance is attributed to the diffusion species in the membrane.

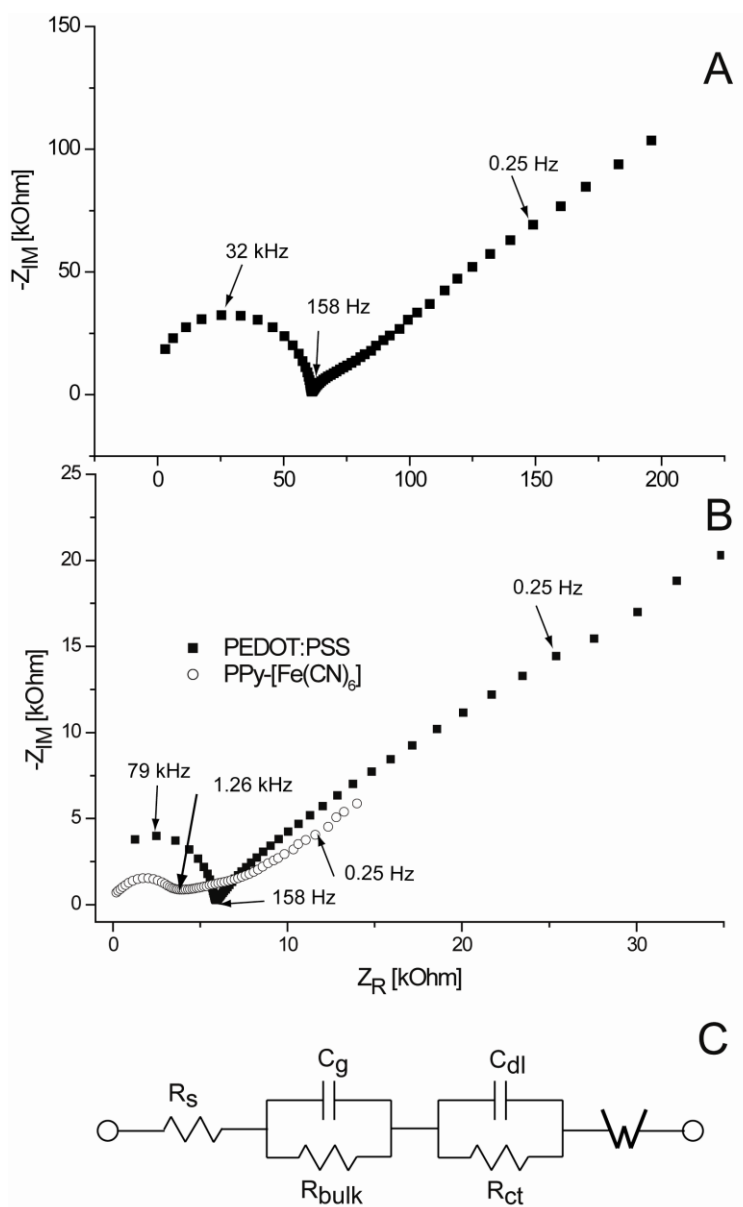


Figure 5.6 Impedance spectra in 0.01M NaCl in presence of 0.01M MgCl₂ background electrolyte (A) The liquid-contact sensor (B) The PPy-Fe(CN)₆ and the PEDOT:PSS solid-contact sensors (C) The equivalent circuit, which was used to fit the impedance spectra.

Table 5.2 Results from impedance measurements (frequency range 100 kHz - 10 mHz)

Inner membrane interface	R_b (kOhm)	C_g (μ F)	R_{ct} (kOhm)	C_{dl} (μ F)	W_R (MOhm)
Liquid	61	7.9×10^{-5}	4.0	14	0.48
PPY-[Fe(CN ₆)]	3	29×10^{-5}	1.2	0.21	0.15
PEDOT:PSS	7	3.1×10^{-5}	5.7	0.24	0.85

The results from the impedance analysis are summarized in Table 5.2. Solution resistance was negligible (<50 Ohm) due to the presence of the background electrolyte. All spectra revealed the presence of a high-frequency semicircle, which can be attributed to the bulk of the PVC membrane with the corresponding bulk resistance and geometric capacitance.

Unfortunately, we have not observed the well-defined low-frequency semicircle that may originate from the interfacial processes at sample/membrane, membrane/IFS, and membrane/CP interfaces. Thus, the reliability of corresponding values of the charge transfer resistance and double layer capacitance are questionable.

Interestingly, the average membrane bulk resistance for solid contact electrodes ($R_b = 8 \pm 2$ kOhm) were smaller than those obtained for liquid contact electrodes ($R_b = 50 \pm 10$ kOhm) with the same membrane composition and thickness (~ 200 μ m). Taking into account the difference in the membrane area (0.08 cm^2 for liquid-contact and 0.28 cm^2 for solid contact sensors) we can calculate the relative bulk resistances as 0.4 kOhm cm^2 and 2.24 kOhm cm^2 respectively. The difference is far greater than what is expected due to the uncertainty in membrane thickness caused by the fabrication process we employed. Similar experimental results were observed earlier,²³ in which a substantial decrease in the resistance corresponding to the high-frequency semicircle was observed upon incorporation of the CP layer into the solid-contact membrane electrode. It leads us to the same conclusion²³ that the high-frequency “bulk”

resistance may indeed include the charge transfer at boundary between membrane and aqueous phase(s), which is significantly lower for the membrane/CP interface.

The influence of the polarization at the CP/membrane interface was examined in PEDOT:PSS based sensors in a solution of 10^{-2} M NaCl, and the results were compared to those for the liquid-contact sensor. A sequence containing 10 current pulses at fixed amplitude of $-6 \mu\text{A}$ with different durations was applied across the membrane. In a series of separate experiments the duration of the applied current pulses was gradually increased from 1 s to 6 s along with the corresponding increase of the duration of the stripping period, which was 15-fold longer than the current pulse. The liquid-contact sensors demonstrated a total potential drift within ± 0.5 mV of the original potential regardless to the duration of the uptake pulse.

In contrast, the results shown in Figure 5.7 revealed that solid-contact PEDOT:PSS sensors exhibit a drastic increase in the total recorded potential drift at certain durations of the current pulse as predicted by the theoretical model. Decreasing the concentration of ETH500 in the membrane from 72 to $16.8 \text{ mmol kg}^{-1}$ caused a potential instability at shorter pulse time as it can be expected according our model. Indeed, the calculated critical value $i \cdot t^{1/2}$ $8.8 \cdot 10^{-5} \text{ A} \cdot \text{s}^{1/2}$ using equation 16 for the ETH500 concentration of 72 mmol kg^{-1} was within the same order of magnitude as the experimental value of $2.4 \cdot 10^{-5} \text{ A} \cdot \text{s}^{1/2}$.

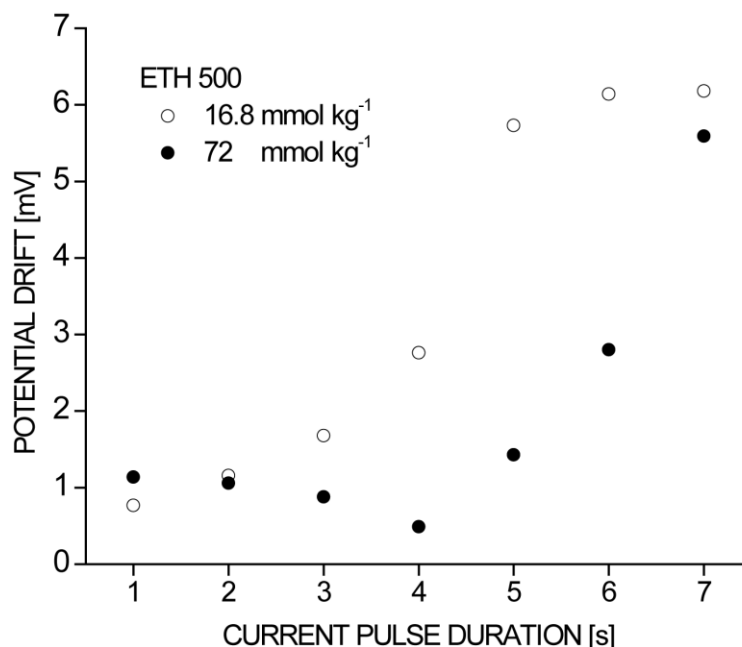


Figure 5.7 The total potential drift of the PEDOT:PSS solid-contact sensor as a function of the duration of the applied current pulse of $-6 \mu\text{A}$ and ETH500 concentration in the membrane.

Due to the fact that the best performance was observed for the sensors with the PEDOT:PSS transduction layer we fabricated protamine-selective pulstrodes on the PEDOT:PSS substrate. The electrode membrane contained a lipophilic salt tetradodecylammonium dinonylnaphthalenesulfonate (TDDA-DNNS). The membrane composition was similar to its liquid-contact counterpart.¹⁵

The recorded time traces for protamine sensor are presented in Figure 5.8. The 1 s current pulses of $-7 \mu\text{A}$ were applied followed by stripping period of 10 s at open circuit potential, which was close to 0 mV. The sensor exhibited a stable and reversible response to protamine within the concentration range of 0.03 to 100 mg L⁻¹ in a solution of 0.1 M NaCl and 50 mmol TRIS-HCl with the pH of 7.40. The observed potential drift did not exceed 0.5 mV min⁻¹. The selectivity of the protamine sensor and influence of the background electrolyte composition was very similar to that reported for its liquid contact counterpart.¹⁵ Addition of 10 mmol of KCl to the

sample did not cause the potential change more than 5 mV. The sensor response function was acceptably reproducible (within ± 2 mV) after the sensor was stored in 0.1 M NaCl solution for 14 days.

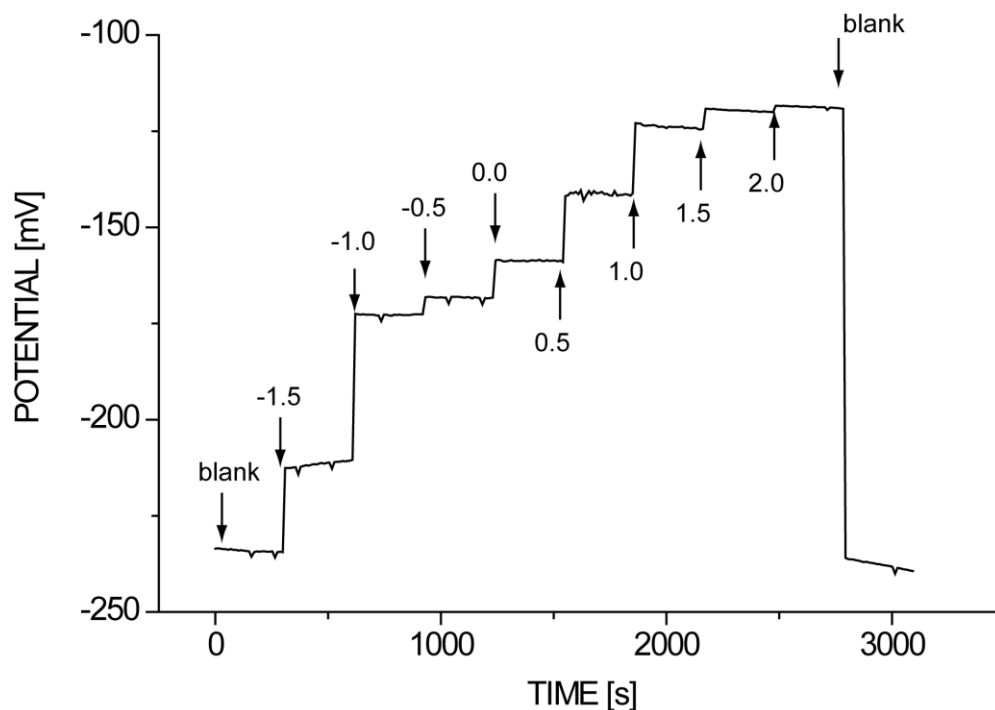


Figure 5.8. Time-dependent response of protamine-selective PEDOT:PSS solid-contact sensor in the solution of 0.1 M NaCl and 50 mmol TRIS, pH 7.40. The numbers represent the $\log C_{\text{protamine}}$ (mg L^{-1}).

The detection limit at 1 s current pulses of $-7 \mu\text{A}$ in a saline solution 0.03 mg L^{-1} was more than an order of magnitude lower than 0.5 mg L^{-1} reported earlier for the liquid-contact protamine sensor at the same current.⁶ This improvement may be attributed to the lower current density used in our experiments. At the same current of $-7 \mu\text{A}$ the membrane area of a CP-based sensor (0.28 cm^2) was larger than that in the liquid-contact sensor (0.08 cm^2).¹⁵ Protamine limiting current ($\approx 1.8 \mu\text{A}$) was calculated according Levich equation¹⁵ using concentration of protamine of $10^{-6} \text{ mol L}^{-1}$, a net charge of 20, a stirring rate of 100 rpm, and an aqueous diffusion coefficient of $10^{-6} \text{ cm}^2/\text{s}$. Lower current of $-7 \mu\text{A}$ used in the experiment was closer to the protamine

limiting current than in the previous experiments^{6, 15} causing less sodium to be extracted into the membrane and, thus, increasing fraction of extracted protamine ions and improving the low detection limit. This is an important indication that the pulsed galvanostatic sensors with polymeric membranes^{5, 6, 14, 15} can be further optimized for better performance.

5.6 Conclusions

Conducting polymers can be successfully used for the fabrication of solid-state pulsed galvanostatic sensors with solvent PVC membranes in order to form a transduction layer between the membrane and electron-conductive substrate. The replacement of the liquid-contact interface with a CP results in the decrease of apparent membrane resistance possibly due to the lowering of charge transfer resistance at the inner membrane interface. The CP/membrane interface exhibited good reversibility under periodic polarization by a constant current in alternating potentiostatic/galvanostatic mode. The sensor incorporating PEDOT:PSS as a conducting polymer showed improved performance over other conducting polymers such as PPy and PPy doped with $\text{Fe}(\text{CN})_6^{3-}$.

However, the simple diffusion-based theoretical model considered here predicts the polarization at the CP/membrane under applied current for the PEDOT:PSS based transduction layer, which can cause the disruption of the sensor response function at relatively small current densities. The experimental results on the limits of potential stability for the PEDOT:PSS based sodium-selective sensor are in relatively good agreement with the theoretical predictions. This may impose a limitation on the development of CP-based solid-contact ion-selective pulsed galvanostatic sensors.

Based on the PEDOT:PSS substrate we developed solid-state reversible polyion-selective sensor with improved low detection limit, which can be used as an end-point detector^{6, 15} for the detection of the anticoagulant heparin via titration with protamine.

The application of protamine sensor for the detection of anticoagulants such as high and low molecular weight heparin is in progress in our research group.

5.7 Acknowledgement

The authors acknowledge the College of Science, the Department of Chemistry at Oregon State University, and the Summer Undergraduate Research program at OSU supported by the Howard Hughes Medical Institute.

5.8 References

- (1) Bakker, E. *Anal. Chem.* **2004**, *76*, 3285-3298.
- (2) Ceresa, A.; Pretsch, E.; Bakker, E. *Anal. Chem.* **2000**, *72*, 2050.
- (3) Fu, B.; Bakker, E.; Yun, J. H.; Yang, V. C.; Meyerhoff, M. E. *Anal. Chem.* **1994**, *66*, 2250-2259.
- (4) Muslinkina, L.; Pretsch, E. *Chem. Comm.* **2004**, 1218-1219.
- (5) Shvarev, A.; Bakker, E. *Anal. Chem.* **2003**, *75*, 4541-4550.
- (6) Shvarev, A.; Bakker, E. *J. Am. Chem. Soc.* **2003**, *125*, 11192-11193.
- (7) Vigassy, T.; Ceresa, A.; Badertscher, M.; Morf, W. E.; Rooij, N. F.; Pretsch, E. *Sens. Actuat. B* **2001**, *76*, 476.
- (8) Xu, Y. D.; De Marco, R.; Shvarev, A.; Bakker, E. *Chem. Comm.* **2005**, 3074-3076.
- (9) Bakker, E., 230th ACS National Meeting **2005**, American Chemical Society, Washington, D.C.
- (10) Bakker, E.; Qin, Y. *Anal. Chem.* **2006**, *78*, 3965-3983.
- (11) Jadhav, S.; Bakker, E. *Anal. Chem.* **2001**, *73*, 80-90.
- (12) Makarychev-Mikhailov, S.; Shvarev, A.; Bakker, E. *J. Am. Chem. Soc.* **2004**, *126*, 10548-10549.
- (13) Makarychev-Mikhailov, S.; Shvarev, A.; Bakker, E. *Anal. Chem.* **2006**, *78*, 2744-2751.
- (14) Shvarev, A.; Bakker, E. *Talanta* **2004**, *63*, 195-200.
- (15) Shvarev, A.; Bakker, E. *Anal. Chem.* **2005**, *77*, 5221-5228.
- (16) Bobacka, J. *Electroanalysis* **2006**, *18*, 7-18.
- (17) Michalska, A. *Electroanalysis* **2005**, *17*, 400-407.
- (18) Michalska, A.; Dumanska, J.; Maksymiuk, K. *Anal. Chem.* **2003**, *75*, 4964-4974.
- (19) Pawlowski, P.; Michalska, A.; Maksymiuk, K. *Electroanalysis* **2006**, *18*, 1339-1346.
- (20) Ramamurthy, N.; Baliga, N.; Wahr, J.; Schaller, U.; Yang, V. C.; Meyerhoff, M. E. *Clin. Chem.* **1998**, 606-613.
- (21) Guo, J. D.; Amemiya, S. *Analytical Chemistry* **2006**, *78*, 6893-6902.
- (22) DeLongehamp, D. M.; Vogt, B. D.; Brooks, C. M.; Kano, K.; Obrzut, J.; Richter, C. A.; Kirillov, O. A.; Lin, E. K. *Langmuir* **2005**, *21*, 11480-11483.
- (23) Cadogan, A.; Gao, Z.; Lewenstam, A.; Ivaska, A. *Anal. Chem.* **1992**, *64*, 2496-2501.
- (24) Meier, P. C. *Anal. Chim. Acta* **1982**, *136*, 363.

- (25) Bradner, F. P.; Shapiro, J. S.; Bowley, H. J.; Gerrard, D. L.; Maddams, W. F. *Polymer* **1989**, *30*, 914-917.
- (26) Nilsson, D.; Chen, M. X.; Kugler, T.; Remonen, T.; Armgarth, M.; Berggren, M. *Adv. Mater.* **2002**, *14*, 51-54.
- (27) Lisowska-Oleksiak, A.; Kazubowska, K.; Kupniewska, A. *J. Electroanal. Chem.* **2001**, *501*, 54-61.
- (28) Penner, R. M.; Van Dyke, L. S.; Martin, C. R. *J. Phys. Chem.* **1988**, *92*, 5274-5282.
- (29) Genies, E. M. B., G.; Diaz, A. F. 1983; 149 *J. Electroanal. Chem.* **1983**, *149*, 101-113.
- (30) Branzoi, V.; Pilan, L.; Ionita, M.; Branzoi, F. *Mol. Cryst. Liq. Cryst.* **2004**, *416*.
- (31) Bakker, E.; Buhlmann, P.; Pretsch, E. *Chem. Rev.* **1997**, *97*, 3083-3132.
- (32) Sokalski, T.; Ceresa, A.; Fibbioli, M.; Zwickl, T.; Bakker, E.; Pretsch, E. *Analytical Chemistry* **1999**, *71*, 1210-1214.
- (33) Cui, X.; Martin, D. C. *Sens. Actuators, B* **2003**, *89*, 92-102.
- (34) Vazquez, M.; Bobacka, J.; Ivaska, A.; Lewenstam, A. *Sensors And Actuators B-Chemical* **2002**, *82*, 7-13.

CHAPTER 6

CONCLUSION AND FUTURE ASPECTS

The main objective of this work is to explore pulstrodes as analytical tools, which can spearhead the integration of sensing devices into clinical laboratory for the testing of physiological samples. Pulstrode was initially introduced as a galvanostatic measuring protocol for ion selective membranes that yield response curves which mimic the traditional ISE behavior, with Nernstian response slopes and selectivities that can be described with Nikolskii equation. It was soon realized that having galvanostatic control over the reversible extraction of ions to the membrane has significant advantages, especially in regard of polyions. Successful protamine and heparin sensing electrodes were developed using this sensing protocol. However, important sensor properties related to the determination of ions of physiological importance have been overlooked.

In this dissertation, important sensor properties including, selectivity improvement, use of new highly selective ionophores and development of solid contact sensors are discussed. In chapter 2, a novel, simple method in determination of unbiased selectivity using pulstrode is introduced. Method of determination of unbiased selectivity by conditioning the membrane with a discriminated ion is reviewed side by side with the new method, to exhibit the validity and compare the ease of the new method.

The primary challenge of the established traditional ISE method is its sensitivity towards the primary ions. Substantial measures have to be taken to avoid membrane exposure to primary ions in order to obtain the unbiased selectivity of discriminated ions. Further, long-term potential drifts have been observed when first exposed to a solution of primary ions.

The method we established herein, unlike its potentiometric counterpart produces unbiased selectivity irrespective of whether it is exposed to the primary ions or not. This characteristic is attributed to the ion selective membrane lacking ion exchanger properties, thus, preventing the transmembrane ion flux. Therefore the novel method should be particularly attractive for clinical analysis where highly improved sensor

selectivity is desired for determination of a particular ion in a highly discriminated background.

Main focus of the chapter 3 is to establish the new method as a general procedure to characterize the carrier based pulstrodes. The general utility of the method is established experimentally with a variety of neutral cation carriers including, K^+ , Ag^+ and Ca^{2+} . Selectivity coefficients determined in here are compared with the results previously reported for the potentiometric ISEs. As a consequence the simplicity and reliability of the introduced method is compared not only with the established method used in chapter 2, but also with the values obtained using, buffered inner filling solution with the complexing agents and solid contact electrodes. Selectivity coefficients we obtained are in good agreement with the literature values and repeatedly demonstrate slight improvements. This could be credited to the suppressed transmembrane ionic flux of the pulstrodes, in comparison to the controlled ionic flux from the membranes of traditional ISEs.

Further sensor selectivity improvement is possible with the incorporation of highly selective ionophores. While classical ion exchanger membranes are still widely used in anion selective membranes, such sensors often suffer from insufficient selectivity. As a consequence anion selective carriers are in high demand. In chapter 4, we introduce MC4 as a highly selective carrier for anions. Unbiased selectivity of this carrier was determined using pulstrodes as well as traditional ISEs. Moreover to better understand the sensing mechanism, potentiometric binding experiments were used to characterize the stoichiometry and complex formation constants of this ionophore. It was found that it formed extremely stable 1:2 complex ($\log \beta_2 = 16.58 \pm 0.282$) and a relatively weak 1:1 ($\log K_1 = 5.33 \pm 0.046$) complex.

Even though no drawbacks of the method we introduced in chapter 2, in determining unbiased selectivity using pulstrodes were encountered when using cationic carriers, a shortcoming was observed when assessing anion carriers. True thermodynamic selectivity of the carrier was not observed for sensor membranes that were exposed to its primary ion. Nevertheless unlike its companion potentiometric method Nernstian

response was obtained for the discriminated ions. Therefore this shortcoming was assumed to be the result of high complex stability observed for the complex. However, further studies are required to come to a definite conclusion.

In order to fully utilize the aforesaid sensor properties in clinical samples, reliable, ideally maintenance free sensors are required. As a consequence we focus our efforts on development of solid contact electrodes with a conducting polymer (CP) transduction layer, in chapter 5. Several CPs were examined to be used as the intermediate transduction layer including PPy doped with Cl⁻, PPy doped with Fe(CN)₆³⁻ and PEDOT:PSS. Selectivity, short-term and long term stability and impedance studies carried out employing Na selective pulstrodes as a model system, demonstrated the pulstrode with PEDOT:PSS as the best candidate. However unlike in liquid inner contact, polarization at the CP/membrane interface has been predicted based on the simple diffusion based model and has been demonstrated experimentally. This could be a potential limitation to the development of solid contact pulstrodes. However, based on the observations, solid state reversible polyion-selective sensor for protamine using PEDOT:PSS as the transduction layer was developed with improved low detection limits.

Clearly there are many interesting paths of inquiry that remain undiscovered with regard to pulstrodes. The phase boundary potential model¹ for classical ISEs, not only allowed one to quantify sensor properties but also helped predicting the outcome of an experiment which inspired innovations in the field. Therefore the importance of constructing a model for pulstrodes, to study its working principle is apparent.

Efforts were taken in order to understand pulstrodes, in terms of underlying theory and working principle. Calibration data were collected in the two modes available, the applied current mode and the zero current mode, for several carriers including H⁺, Na⁺ and Ca²⁺. The experimental results obtained, presented in Appendix, could not be explained by the simple diffusion model available. This is anticipated since when current is passed through a membrane, ion flux inside the membrane is governed by

diffusion as well as migration. Therefore future work will proceed towards obtaining a theoretical model that is capable in reproducing the experimental response.

Though, key application discussed for pulstrodes has been the development of reversible sensors for highly charged polyions, many other sensing principles may be developed in the future, since the tools are now capable in fabricating reversible sensors on the basis of otherwise irreversible reactions.

Reference

- (1) Mathison, S.; Bakker, E. *Anal. Chem* **1998**, *70*, 303-309.

APPENDIX A

EVALUATION OF THE EFFECT OF APPLIED CURRENT ON CATION RESPONSE

To evaluate the effect of current on calibration of different cations, data were collected using Na^+ , Ca^{2+} and H^+ selective pulstrodes. Conventional three electrode setup was used for the measurements. A platinum cage was used as a counter electrode and a double junction Ag/AgCl electrode was used as a reference electrode. While H^+ pulstrodes were tested in universal buffer solution, Na^+ and Ca^{2+} was tested in backgrounds of 10 mM MgCl_2 and 10 mM KCl , respectively. A modified²² AFCBP1 bipotentiostat (Pine Instruments, Grove City, MA) controlled by a PCI-6221 data acquisition board and Lab View 7.1 software (National Instruments, Austin, TX) on a PC was used for measurements. Detailed description on the experimental procedure that is used to obtain the potential response is presented in Chapter 2. Resulting slopes that correspond to calibration plots were plotted against the corresponding applied current.

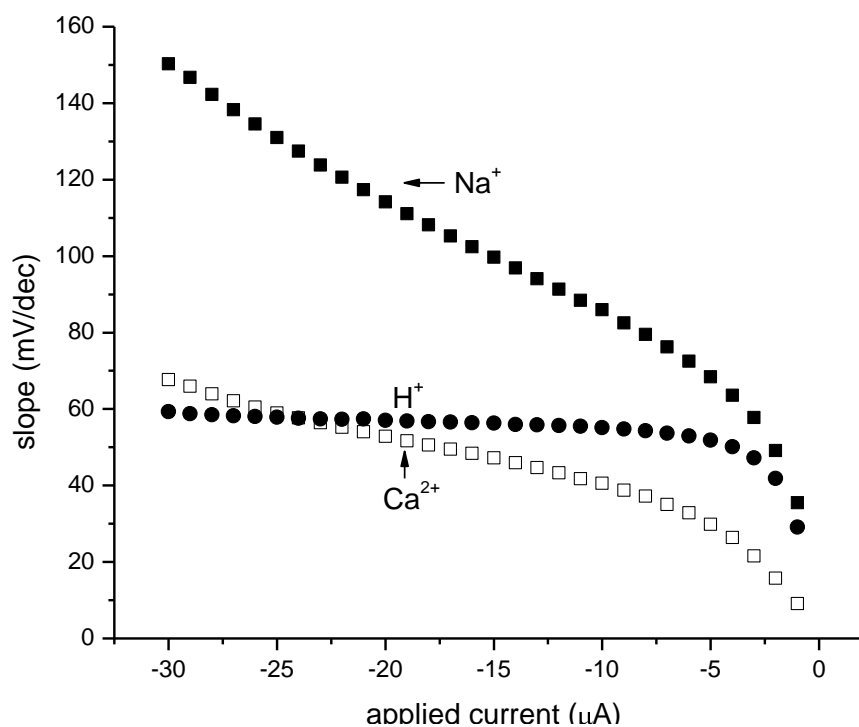


Figure A.1 Slopes obtained for the calibration curves of Na^+ , Ca^{2+} and H^+ pulstrodes, at different currents as a function of the applied current.

As seen in the Figure A.1, Na^+ , Ca^{2+} exhibit an increase in slope of the calibration curve as a function of the applied current. However, the increments are less for Ca^{2+} than for Na^+ . If observed closely, it is apparent, that at a specific current calibration slope obtained for Na^+ is as twice as Ca^{2+} calibration slope. Nevertheless as shown in Figure A.1, slope obtained for the calibration curve of H^+ remains constant and Nernstian.

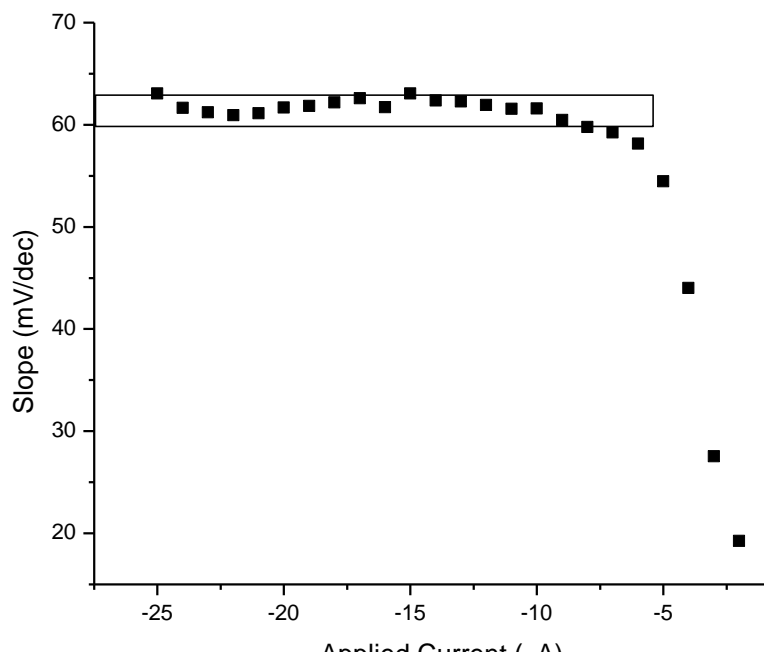


Figure A.2 Slope obtained for calibration plot of ionophore free pulstrode membrane as a function of the applied current

An additional experiment was carried out with a pulstrode membrane carrying no ionophores. The obtained calibration plot slopes are presented in Figure A.2. Experiments carried out with ionophore free membrane, allows to predict that the greater influence towards the super-Nernstian slope comes from the ion-ionophore complex migration & / diffusion into the ion selective membrane.